Physica D 420 (2021) 132869

Contents lists available at ScienceDirect

Physica D

journal homepage: www.elsevier.com/locate/physd

Dynamics of the Tyson–Hong–Thron–Novak circadian oscillator model

Shuang Chen [a,b], Jinqiao Duan [c,*], Ji Li [a]

[a] School of Mathematics and Statistics, Huazhong University of Sciences and Technology, Wuhan, Hubei 430074, PR China
[b] Center for Mathematical Sciences, Huazhong University of Sciences and Technology, Wuhan, Hubei 430074, PR China
[c] Department of Applied Mathematics, Illinois Institute of Technology, Chicago, IL 60616, USA

ARTICLE INFO

Article history:
Received 18 August 2020
Received in revised form 5 January 2021
Accepted 18 January 2021
Available online 27 February 2021
Communicated by J. Dawes

Keywords:
Circadian oscillator
Canard explosion
Relaxation oscillation
Saddle–node bifurcation
Birhythmicity

ABSTRACT

We study the dynamics of a circadian oscillator model proposed by Tyson, Hong, Thron and Novak. This model describes a molecular mechanism for the circadian rhythm in Drosophila. After giving a detailed study of its equilibria, we investigate the dynamics in the cases that the rate of mRNA degradation is sufficiently high or low. When the rate is sufficiently high, we prove that there are no periodic orbits in the region with biological meaning. When the rate is sufficiently low, this model is transformed into a slow–fast system. Then based on the geometric singular perturbation theory, we prove the existence of relaxation oscillations, canard explosion, saddle–node bifurcations, and the coexistence of two limit cycles in this model. These results are helpful to understand the effects of biophysical parameters on circadian oscillations. Finally, we give the biological interpretation of the results and point out that this model can be transformed into a Liénard-like equation, which could be helpful to investigate the dynamics of the general case.

1. Introduction

Circadian rhythms of physiology and behavior with a period about 24 h have been found in many organisms, for example, in fruit flies, plants and vertebrate animals. These circadian clocks allow us to adapt to the alternation of day and night. In order to grasp the mechanisms for the generation of circadian rhythms, numerous theoretical models ranging from generic autonomous oscillators to molecular-based models have been proposed in the past tens of years. See, for example, [1–5] and references therein.

Drosophila has a molecular circadian oscillation which has been modeled to understand the mechanisms for circadian rhythms. The classical mechanism is that the clock proteins (PER and TIM) dimerize and then inhibit the transcription of their clock genes. Thus many models are based on a negative feedback loop. In order to describe the multiple states of clock proteins and clock genes, these models are always high-dimensional systems of ordinary differential equations [1,4,5]. The complexity of these systems causes a major obstacle to analyzing the underlying mechanisms for circadian oscillations.

Motivated by the experimental discoveries on PER phosphorylation and proteolysis in [6,7], Tyson, Hong, Thron and Novak [8] proposed a positive feedback loop to the circadian oscillator in Drosophila, which was based on the stabilization of PER upon its dimerization with TIM. See [8, Figure 1, p.2412] for the molecular mechanism. To grasp the importance of positive feedback and keep the model as simple as possible, Tyson, Hong, Thron and Novak in [8] set up a three-dimensional circadian oscillator model

$$\begin{aligned}\frac{dM}{dt} &= \frac{v_m}{1+(P_2/P_c)^2} - k_m M,\\ \frac{dP_1}{dt} &= v_p M - \frac{k_1 P_1}{J_p + P_1 + rP_2} - k_3 P_1 - 2k_a P_1^2 + 2k_d P_2,\\ \frac{dP_2}{dt} &= k_a P_1^2 - k_d P_2 - \frac{k_2 P_2}{J_p + P_1 + rP_2} - k_3 P_2,\end{aligned} \tag{1.1}$$

where the system states M, P_1 and P_2 denote the concentration of mRNA, protein monomer and protein dimer, respectively. The biological descriptions of the model parameters are shown in Table 1 (see also in [8, Table 1]). Let the ratio $r = 2$ and $k_1 > k_2$. Consider the change of the total protein $P = P_1 + 2P_2$. Then (1.1) is converted into

$$\begin{aligned}\frac{dM}{dt} &= \frac{4v_m P_c^2}{4P_c^2 + (P - P_1)^2} - k_m M,\\ \frac{dP}{dt} &= v_p M - \frac{(k_1 - k_2)P_1 + k_2 P}{J_p + P} - k_3 P,\\ \frac{dP_1}{dt} &= v_p M - \frac{k_1 P_1}{J_p + P} - k_3 P_1 - 2k_a P_1^2 - k_d P_1 + k_d P.\end{aligned} \tag{1.2}$$

Assume that the dimerization reactions k_a and k_d are sufficiently large compared to other rate parameters, Tyson, Hong, Thron and Novak [8] applied the quasi-steady-state approximation (see, for

* Corresponding author.
E-mail addresses: schen@hust.edu.cn (S. Chen), duan@iit.edu (J. Duan), liji@hust.edu.cn (J. Li).

https://doi.org/10.1016/j.physd.2021.132869
0167-2789/

Table 1
The biological descriptions of the model parameters.

Parameter	Biological description
v_m	The maximum rate of mRNA synthesis
k_m	The first-order rate of mRNA degradation
P_c	The value of dimer at the half-maximum transcription rate
v_p	The rate for translation of mRNA into the monomer
k_1	The maximum rate for monomer phosphorylation
k_2	The maximum rate for dimer phosphorylation
k_3	The first-order degradation rate of the monomer and dimer
J_P	The Michaelis constant for protein kinase DBT
k_a	The rate of dimerization
k_d	The rate of dissociation of the dimer
r	The ratio of enzyme–substrate dissociation constants for the monomer and dimer

instance, [9,10]) to reduce the three-dimensional system (1.2) into a simpler two-dimensional system

$$\begin{aligned} \frac{dM}{dt} &= \frac{4v_m P_c^2}{4P_c^2 + (P - h(P))^2} - k_m M, \\ \frac{dP}{dt} &= v_p M - \frac{(k_1 - k_2)h(P) + k_2 P}{J_p + P} - k_3 P, \end{aligned} \tag{1.3}$$

where the constant $K = k_a/k_d$ and the function h is given by

$$h(P) = \frac{\sqrt{1 + 8KP} - 1}{4K}, \qquad P \geq 0.$$

Here system (1.3) is called the two-dimensional Tyson–Hong–Thron–Novak circadian oscillator model (the THTN model for short). Indeed, under the same assumptions as in [8], our recent work [11] proved that the three-dimensional system (1.2) possesses a two-dimensional invariant manifold, which is also a global attractor in the region with biological meaning. Furthermore, the vector field on this invariant manifold has an expansion with respect to a small parameter and its zero-order approximation is the THTN model. So the dynamics of (1.2) can be effectively approximated by the THTN model.

The THTN model is a simplified two-dimensional system, but [8] found that it also generates oscillations and naturally illustrates several properties of circadian rhythms, such as temperature compensation. On the other hand, the THTN model has an advantage in theoretical analysis over high-dimensional models: the phase plane analysis is applicable to detect its oscillations. However, there are still two obstacles in analyzing its dynamics, that is, it possesses multiple parameters and is topologically equivalent to a high-order polynomial system. In order to explore the properties of the THTN model, Tyson et al. [8] numerically studied the periods of limit cycles by varying (K, k_1) and fixing other parameters, and found that it has a limit cycle with a period of about 24 h in a large parameters domain of (K, k_1). Simon and Volford [12] used the parametric representation method to study the properties of equilibria and bifurcation curves by varying (v_p, k_1). Goussis and Najm [13] numerically compared the differences of periodic solutions in the original system (1.1) and the THTN model. Jiang et al. [14] numerically studied the effects of several model parameters on the periods of circadian oscillations, and pointed out that it is reasonable to apply the THTN model to study the periodic behaviors in the original system (1.1).

We are interested in the effects of the biophysical parameters on the periodic behaviors in the THTN model. These results are determined by the dynamics of the THTN model, and allow us to understand the roles of proteolysis and dimerization of clock proteins in generating circadian rhythms. Noting that mRNA degradation plays a pivotal role in eukaryotic gene expression, we then focus on the cases that the rate of mRNA degradation is sufficiently high or low. The dynamics of the THTN model with general k_m is a more complicated problem, and will be studied in future work. In the final section, we point out that the THTN model is topologically equivalent to a Liénard-like equation. This structure is helpful to study the global dynamics of the THTN model with general k_m and the effects of the biophysical parameters on the periods of circadian oscillators.

When the rate of mRNA degradation is sufficiently high, this case is called the high degradation rate case for simplicity. We first obtain the existence of a bounded attractor by applying Gronwall's Inequality. Then we further prove that there are no periodic orbits in the THTN model and all orbits starting from the initial values in the domain with biological meaning are attracted to locally stable foci or nodes, except for the stable manifolds of saddles. See Theorem 4.1. This indicates that circadian oscillations require the rate of mRNA degradation to be bounded, and could disappear when this rate is high.

Relaxation oscillations and canard explosions were found in many circadian models [2,4] and have not yet been considered in the THTN model. These phenomena typically appear in a planar slow–fast system. We give a detailed study of these oscillations for the THTN model and are also motivated by the numerical simulations in [8]. For example, [8, Figure 2] showed that the time evolution of the concentration of mRNA exhibits an apparent slow–fast structure. The limit cycle in [8, Figure 3A] looks like a relaxation oscillation. [8] numerically found that for $K < 50$, the period of limit cycle abruptly increases and becomes quite sensitive to the changes of parameters. The similar phenomenon appears in canard explosion.

The slow–fast structure for the THTN model in the present paper is induced by the low rate of mRNA degradation, which is referred to as the low degradation rate case. To analyze relaxation oscillations and canard explosions, one efficient approach is to apply the geometric singular perturbation theory (see [15–21]). For convenience, we introduce its basic notions in Section 2. In slow–fast systems with S-shaped critical manifolds, the shapes of perturbed limit cycles depend on the types of two non-hyperbolic points. If a non-hyperbolic point is also an equilibrium of the slow–fast THTN model, then it is a canard point. Otherwise, it is a jump point (see Section 5). So one of key steps is to give a complete classification of all possible distributions of the equilibria (see Lemma 3.3) and then distinguish the types of them. After that, we obtain the desired circadian oscillators in the form of canard cycles and relaxation oscillations by the normal forms near the canard points and the results in [18,19,22]. See Theorems 5.1, 5.3 and 5.4.

Besides these oscillations, we study several interesting phenomena on the dynamics of the THTN model. For example, by the Fenichel Theorem [22, Theorem 9.1], we prove the nonexistence of limit cycles, and the existence of homoclinic orbits and heteroclinic orbits. See Theorems 5.1, 5.3 and 5.4. Based on the center manifold theory, we study the saddle–node bifurcations near saddle–node points. See Theorem 5.2. We also prove the coexistence of two limit cycles for the THTN model in some parameter domains, where one is stable and the other is unstable. See **(vi)** of Theorem 5.1. The interesting occurrence of two different limit

cycles for some parameters is referred to as birhythmicity. This phenomenon suggests that the periods of oscillations depend on environment conditions. The coexistent limit cycles found in the THTN model are different from those in the negative feedback model proposed by Leloup and Goldbeter [5], which numerically showed the coexistence of two stable limit cycles.

This paper is organized as follows. In Section 2, we introduce basic notions on geometric singular perturbation theory as preparations. In Section 3, we provide a complete classification of the equilibria. In Sections 4 and 5 , we analyze the dynamics of the THTN model in the high degradation rate case and the low degradation rate case, respectively. We end with some remarks on the further study in the final section.

2. Geometric singular perturbation theory

Multiple time scale systems frequently appear in many practical applications, such as population dynamics [23–27], cellular physiology [28–32], mechanical systems [33–36] and stochastic dynamics [37–40]. These systems usually admits a clear separation in two time scales, one slow time scale and one fast time scale, which are also called the slow–fast systems. Following the pioneering work [22] of Fenichel in 1979, geometric singular perturbation theory has been developed to be an efficient method to study multiple time scale dynamics.

Now we introduce basic notions on geometric singular perturbation theory for planar slow–fast systems. Consider a planar slow–fast system of the form

$$\begin{aligned} \frac{dx}{dt} &= x' = f(x, y, \mu, \varepsilon), \\ \frac{dy}{dt} &= y' = \varepsilon g(x, y, \mu, \varepsilon), \end{aligned} \tag{2.1}$$

where $(x, y) \in \mathbb{R}^2$, $\mu \in \mathbb{R}^m$ with $m \geq 1$, a small parameter ε with $0 < \varepsilon \ll 1$, and the functions f and g are C^k with $k \geq 3$. Letting $\tau = \varepsilon t$, system (2.2) is rescaled to

$$\begin{aligned} \varepsilon \frac{dx}{d\tau} &= \varepsilon \dot{x} = f(x, y, \mu, \varepsilon), \\ \frac{dy}{d\tau} &= \dot{y} = g(x, y, \mu, \varepsilon). \end{aligned} \tag{2.2}$$

In the limiting case $\varepsilon = 0$, system (2.1) becomes the layer equation

$$\begin{aligned} x' &= f(x, y, \mu, 0), \\ y' &= 0, \end{aligned} \tag{2.3}$$

and system (2.2) becomes the reduced equation

$$\begin{aligned} 0 &= f(x, y, \mu, 0), \\ \dot{y} &= g(x, y, \mu, 0). \end{aligned} \tag{2.4}$$

For the layer equation (2.3) with a fixed $\mu \in \mathbb{R}^m$, its equilibria set $\mathcal{C}_{\mu,0} := \{(x, y) \in \mathbb{R}^2 : f(x, y, \mu) = 0\}$ is the phase state of the reduced equation (2.4). A point in $\mathcal{C}_{\mu,0}$ with $\partial f/\partial x \neq 0$ is called a regular point. Otherwise it is called a contact point. The set $\mathcal{C}_{\mu,0}$ is called the critical set and is called the critical manifold if it is a submanifold of $\mathbb{R}^2$. This set is useful in investigating the dynamics of the slow–fast system (2.1). More specifically, by the Fenichel theory [22], a normally hyperbolic manifold $\mathcal{M}_{\mu,0}$, which is a compact submanifold $\mathcal{C}_{\mu,0}$ formed by regular points of a critical set $\mathcal{C}_{\mu,0}$, is perturbed to a slow manifold $\mathcal{M}_{\mu,\varepsilon}$ of slow–fast system (2.1) with $0 < \varepsilon \ll 1$. The stable and unstable manifolds of $\mathcal{M}_{\mu,0}$ are also persistent for a sufficiently small ε.

The preceding results show the dynamics near the normally hyperbolic invariant manifolds. However, non-hyperbolic points at which $\partial f/\partial x = 0$ widely appear in applications, such as the well-known van der Pol equation. A contact point arising in a critical manifold is one of the most common forms for the breakdown of normal hyperbolicity. We analyze two different contact points in planar slow–fast systems, that is, the so-called jump point and canard point [15,18,41], which can induce relaxation oscillation and canard cycle, respectively. Roughly speaking, the reduced flow (2.4) directs towards a jump point and passes through a canard point. Relaxation oscillations and canard cycles can be seen as the perturbations of slow–fast cycles formed by gluing the orbits of the reduced system and the layer equations. Four classical slow–fast cycles are shown in Fig. 1.

Relaxation oscillations, which perturb from their singular counterparts (see Fig. 1(d)), are periodic solutions which spend a long time along the slow manifold towards a jump point, jumps from this contact point, spends a short time parallel to the unstable fibers towards another stable branch of the critical manifold, follows the slow motion again until another jump point is reached, and finally forms a closed loop via several similarly successive motions [19,42]. Canard cycle appearing near a canard point is a periodic solution which is contained in the intersection of an attracting slow manifold and a repelling slow manifold [15,19,41]. This phenomenon is closely related to canard explosion [19,41], which is a transition from a small limit cycle of Hopf type via a family of canard cycles to a relaxation oscillation.

3. Model reduction and analysis of equilibria

In order to simplify calculations, we first transform the THTN model into an equivalent system and then consider the properties of its equilibria. Letting

$$(M, P, t) \ \rightarrow \ \left(\frac{k_3}{8K\nu_p} y, \frac{1}{8K} x, \frac{1}{k_3} t\right),$$

the THTN model is transformed into

$$\begin{aligned} \frac{dx}{dt} &= x' = y - \psi_1(x), \\ \frac{dy}{dt} &= y' = \varepsilon \left(\psi_2(x) - y\right), \end{aligned} \tag{3.1}$$

where

$$\begin{aligned} &\psi_1(x) = \frac{b_1\phi(x) + b_2 x}{a + x} + x, \quad \psi_2(x) = \frac{v}{c + (x - \phi(x))^2}, \\ &\phi(x) = 2(\sqrt{1 + x} - 1), \qquad x \geq 0, \end{aligned} \tag{3.2}$$

and the positive parameters $a, b_1, b_2, c, \varepsilon, v$ are given by

$$\begin{aligned} &a = 8J_P K, \quad b_1 = \frac{8(k_1 - k_2)K}{k_3}, \quad b_2 = \frac{8k_2 K}{k_3}, \\ &c = 256K^2 P_c^2, \quad \varepsilon = \frac{k_m}{k_3}, \quad v = \frac{2048\nu_m \nu_p P_c^2 K^3}{k_3 k_m}. \end{aligned}$$

Throughout this paper, we assume that the rate of mRNA degradation is proportional to that of mRNA synthesis. Then the parameters v and ε are independent of each other.

Define the function ψ by

$$\psi(x) := \psi_1(x) - \psi_2(x) \quad \text{for} \quad x \geq 0. \tag{3.3}$$

Concerning ψ_i and ψ, we have the following two lemmas.

Lemma 3.1. *Let ψ_1 be defined by (3.2). Then the second derivative ψ_1'' of ψ_1 has a unique positive zero $x_+ = u_+^2 + 2u_+$, where u_+ is the unique positive zero of the function ϕ_1 defined as*

$$\begin{aligned} \phi_1(u) = {} & 3b_1(u + 1)^4 - (8b_1 + 4ab_2)(u + 1)^3 + 6b_1(1 - a)(u + 1)^2 \\ & - b_1(a - 1)^2, \end{aligned} \tag{3.4}$$

and the following statements hold:

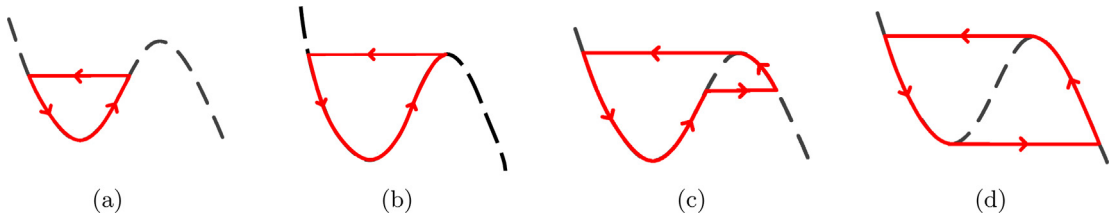

Fig. 1. 1(a) Canard slow–fast cycle without head. 1(b) Transitory canard. 1(c) Canard slow–fast cycle with head. 1(d) Singular relaxation cycle.

(i) $\psi_1(0) = 0$, $\psi_1(x) > 0$ *for* $x > 0$ *and* $\psi_1(x)/x \to 1$ *as* $x \to +\infty$.

(ii) $\psi_1'(0) = (b_1 + b_2)/a + 1$, $\psi_1'(x) \to 1$ *as* $x \to +\infty$ *and* ψ_1' *admits the following trichotomies:*

(ii.1) *if* $\psi_1'(x_+) > 0$, *then* $\psi_1'(x) > 0$ *for* $x \geq 0$.

(ii.2) *if* $\psi_1'(x_+) = 0$, *then* $\psi_1'(x) \geq 0$ *for* $x \geq 0$, *and* x_+ *is the unique positive zero of* ψ_1'.

(ii.3) *if* $\psi_1'(x_+) < 0$, *then* ψ_1' *has exactly two zeros* x_m *and* x_M *with* $0 < x_m < x_+ < x_M$, *and* ψ_1' *satisfies that* $\psi_1'(x) > 0$ *for* $0 < x < x_m$ *and* $x > x_M$, $\psi_1'(x) < 0$ *for* $x_m < x < x_M$.

(iii) $\psi_1''(x) < 0$ *for* $x \in [0, x_+)$ *and* $\psi_1''(x) > 0$ *for* $x \in (x_+, +\infty)$.

Proof. Set $u = \sqrt{1+x} - 1$ for $x \geq 0$. Then $x = u^2 + 2u$ for $u \geq 0$. By a direct computation,

$$2(u+1)^3(u^2+2u+a)^3\psi_1''(x(u)) = \phi_1(u),$$

where ϕ_1 is defined by (3.4). Then by a standard analysis, we obtain this lemma. □

In **(i)** of Theorem 4.1 we will see that the dynamics of (3.1) with $\psi_1'(x_+) \geq 0$ are simple. Consequently, with no confusion, we always assume that $\psi_1'(x_+) < 0$. So the graph of ψ_1 is S-shaped.

Lemma 3.2. *Let the functions* ψ_2 *and* ψ *be defined by* (3.2) *and* (3.3), *respectively. Then the function* ψ_2 *has the following properties:*

(i) $\psi_2(0) = v/c$, $0 < \psi_2(x) \leq v/c$ *for* $x \geq 0$, *and* $\psi_2(x) \to 0$ *as* $x \to +\infty$.

(ii) $\psi_2'(0) = 0$, $-v/(c\sqrt{c}) \leq \psi_2'(x) < 0$ *for* $x > 0$, *and* $\psi_2'(x) \to 0$ *as* $x \to +\infty$.

(iii) *the second derivative* ψ_2'' *of* ψ_2 *has exactly one zero* $x_1 \in (0, +\infty)$, *which is the unique positive root of equation* $6(\sqrt{x+1}-1)^5 + 5(\sqrt{x+1}-1)^4 - 2c\sqrt{x+1} - c = 0$, *and* $\psi_2''(x) < 0$ *for* $0 < x < x_1$ *and* $\psi_2''(x) > 0$ *for* $x > x_1$.

And the function ψ *has the following properties:*

(iv) *for each positive parameters* a, b_1, b_2, c, ε *and* v, *the function* ψ *has at least one positive zero and at most three positive zeros.*

(v) *if the function* ψ *has precisely two positive zeros* $x = \widetilde{x}_0$ *and* $x = \widetilde{x}_1$ *with* $\widetilde{x}_0 < \widetilde{x}_1$, *then either* $\omega = \widetilde{x}_0$ *or* $\omega = \widetilde{x}_1$ *satisfies that* $\psi(\omega) = \psi'(\omega) = 0$ *and* $\psi''(\omega) \neq 0$.

Proof. By a standard analysis, the properties of ψ_2 are obtained. Hence the proof is omitted.

To obtain the properties on ψ, let $u = \sqrt{1+x} - 1$ for $x \geq 0$. Then

$$\begin{aligned}&(u^2+2u+a)(u^4+a)\psi(x(u))\\ &\quad = (u^4+4u^3+(a+b_2+4)u^2+2(a+b_1+b_2)u)(u^4+c)\\ &\qquad - v(u^2+2u+a) := \phi_2(u).\end{aligned}$$

Since $\phi_2(0) = -av < 0$ and $\phi_2(u) \to +\infty$ as $u \to +\infty$, by continuity there exists at least one positive zero for the function ψ. Note that the third derivative of ϕ_2 is in the form

$$\begin{aligned}\phi_2^{(3)}(u) = {}& 336u^5 + 840u^4 + 120(a+b_2+4)u^3\\ &+ 120(a+b_1+b_2)u^2 + 24cu + 24c,\end{aligned}$$

and $\phi_2^{(3)}(u) > 0$ for $u \geq 0$. Then ϕ has at most three positive zeros. So we have **(iv)**. By studying the properties of ϕ_2, we obtain **(v)**. Therefore, the proof is now complete. □

Assume that $\psi_1'(x_+) < 0$. Then the graph of the function ψ_1 is S-shaped. To consider the properties of the equilibria in (3.1), let $L = L^0 \cup L^1$, $R = R^0 \cup R^1$ and $M = \{(x, y) : y = \psi_1(x), x_m < x < x_M\}$, where the sets

$$\begin{aligned}L^0 &= \{(x_m, \psi_1(x_m))\}, \quad L^1 = \{(x, y) : y = \psi_1(x),\ 0 \leq x < x_m\},\\ R^0 &= \{(x_M, \psi_1(x_M))\}, \quad R^1 = \{(x, y) : y = \psi_1(x),\ x > x_M\}.\end{aligned}$$

We now define symbolic sequences to indicate the numbers and relative positions of the equilibria on the graph of ψ_1. We use, for example, the symbolic sequence LMR to represent that ψ_2 intersects ψ_1 at points in the sets L, M and R in order as the independent variable x increases, other symbolic sequences are similarly defined. These symbolic sequences are referred to as the intersection point sequences.

We next consider all possible intersection point sequences in the case $\psi_1'(x_+) < 0$, which is useful in the proof for the main results in the low degradation rate case.

Lemma 3.3. *Suppose that the function* ψ_1 *satisfies* $\psi_1'(x_+) < 0$, *where the function* ψ_1 *and the constant* x_+ *are defined as in Lemma* 3.1. *Then the intersection point sequences have the following different types (see Fig.* 2*):*

(i) *if the number of the intersection points is one, then all possible intersection point sequences are* L^0, L^1, M, R^0 *and* R^1.

(ii) *if the number of the intersection points is two, then all possible intersection point sequences are* L^0M, L^1M, MM, MR^0 *and* MR^1.

(iii) *if the number of the intersection points is three, then all possible intersection point sequences are* L^0MR^0, L^0MR^1, L^1MR^0, L^1MR^1, L^0MM, L^1MM, MMM, MMR^0 *and* MMR^1.

We give the lengthy proof for this lemma in Appendix A.

4. Dynamics of the high degradation rate case

In this section, we give a detailed study of the dynamics of the THTN model in the high degradation rate case, that is, the rate of mRNA degradation is high enough. Then ε is sufficiently large.

Lemma 4.1. *Let the sets* $\mathbb{R}^2_+$ *and* $\mathcal{A}$ *be respectively defined by* $\mathbb{R}^2_+ = \{(x, y) \in \mathbb{R}^2 : x \geq 0, y \geq 0\}$ *and*

$$\mathcal{A} = \left\{(x, y) \in \mathbb{R}^2 : 0 \leq x \leq \frac{v}{c},\ \ 0 \leq y \leq \frac{v}{c}\right\}.$$

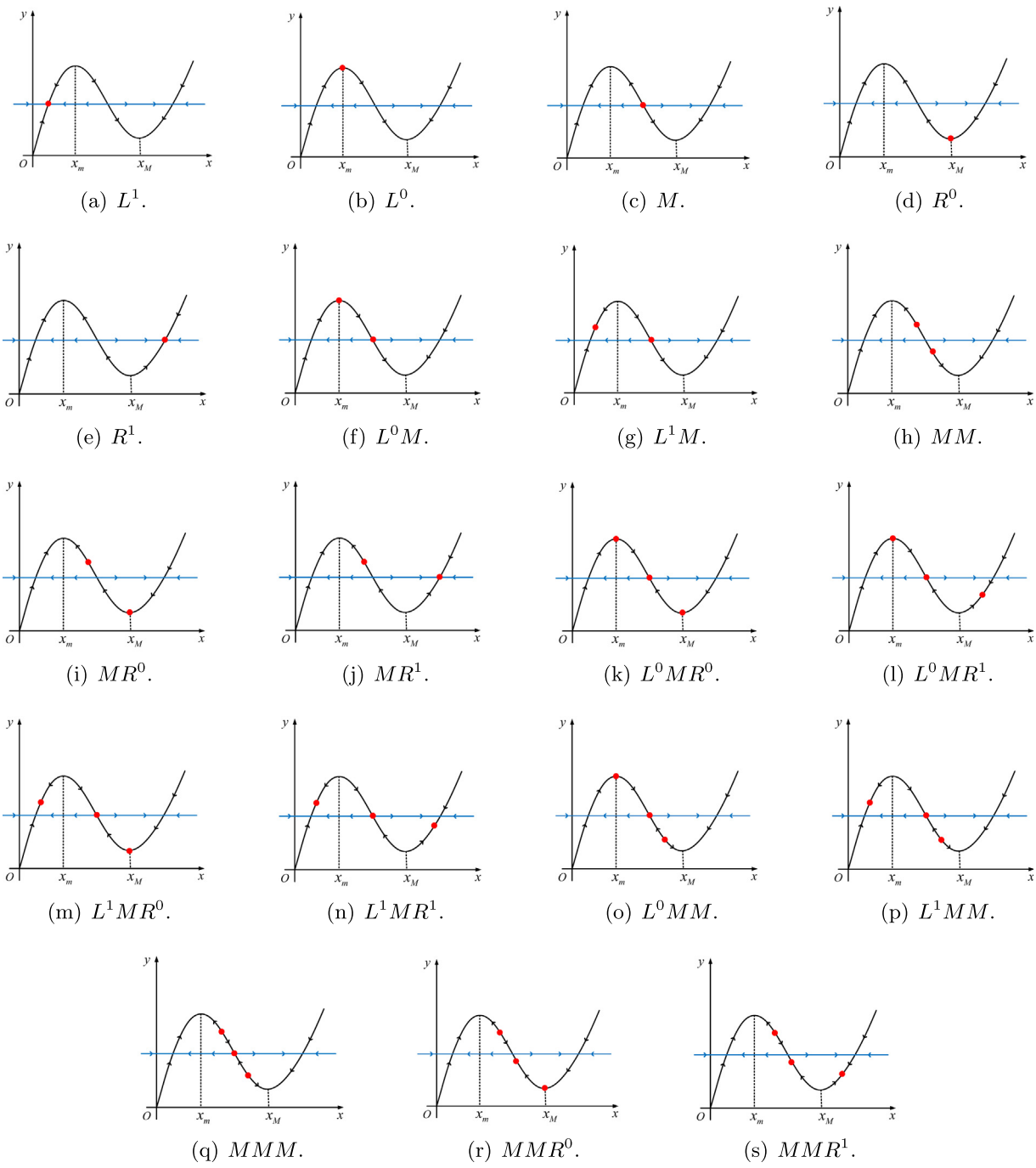

Fig. 2. All possible intersection point sequences and the corresponding slow–fast limits. Red dots are the equilibria lying on the graph of the function ψ_1 (black curve). Black arrows indicate the flow of the reduced equation. Blue arrows indicate the flow of the layer equation.

Then the sets $\mathbb{R}^2_+$ and $\mathcal{A}$ are both the positive invariant sets of system (3.1). Furthermore, the set $\mathcal{A}$ attracts the set $\mathbb{R}^2_+$ under the flow of system (3.1).

Proof. By analyzing the field vector of system (3.1) along the boundaries of the sets $\mathbb{R}^2_+$ and $\mathcal{A}$, the first statement is obtained. For each solution $(x(t), y(t))$ of system (3.1) with the initial value $(x(0), y(0)) \in \mathbb{R}^2_+$, we have that $x(t) \geq 0$ and $y(t) \geq 0$ for $t \geq 0$. Then by the second equation in system (3.1), we have that $y'(t) \leq -\varepsilon y + v/c$ for $t \geq 0$, which together with Gronwall's Inequality yields that

$$y(t) \leq y(0)e^{-\varepsilon t} + v/c, \qquad t \geq 0. \tag{4.1}$$

Consider the first equation in system (3.1) with $0 \leq y(t) \leq v/c$. Similarly, we have that

$$x(t) \leq x(0)e^{-t} + v/c, \qquad t \geq 0. \tag{4.2}$$

Then by (4.1) and (4.2), the second statement holds. Therefore, the proof is now complete. □

Let the point (x_0, y_0) with $x_0 \geq 0$ be a finite equilibrium of system (3.1). Then by the form of system (3.1), the value of x_0 is independent of the parameter ε and only relies on the parameters a, b_i, c and v. In order to obtain the type of equilibrium (x_0, y_0), we consider the Jacobian matrix $\mathcal{J}(x_0, y_0)$ of system (3.1)

at (x_0, y_0)

$$\mathcal{J}(x_0, y_0) = \begin{pmatrix} -\psi_1'(x_0) & 1 \\ \varepsilon\psi_2'(x_0) & -\varepsilon \end{pmatrix}.$$

The determinant and the trace of this Jacobian matrix are respectively given by

$$\mathcal{D}(x_0, y_0) := \varepsilon(\psi_1'(x_0) - \psi_2'(x_0)), \quad T(x_0, y_0) := -\varepsilon - \psi_1'(x_0). \tag{4.3}$$

To determine the type of this equilibrium, we need to further consider the sign of the constant

$$\Delta(x_0, y_0) := (T(x_0, y_0))^2 - 4\mathcal{D}(x_0, y_0) = (\varepsilon - \psi_1'(x_0))^2 + 4\varepsilon\psi_2'(x_0). \tag{4.4}$$

Based on Bendixson's Theorem (see [43, Theorem 7.10, p. 188]), we have the following statements.

Theorem 4.1. *Consider system (3.1). Then the following conclusions hold:*

- **(i)** *if ψ_1 satisfies $\psi_1'(x_+) \geq 0$, then there exists a unique equilibrium (x_0, y_0) in $\mathbb{R}^2_+$, which is a stable focus or node. Furthermore, system (3.1) has no periodic orbits in $\mathbb{R}^2_+$, and (x_0, y_0) attracts the set $\mathbb{R}^2_+$ under the flow of system (3.1).*
- **(ii)** *if ψ_1 satisfies $-\varepsilon < \psi_1'(x_+) < 0$, then system (3.1) has no periodic orbits in $\mathbb{R}^2_+$, and at least one equilibrium and at most three equilibria. Furthermore, the equilibria of system (3.1) admit the following trichotomies:*
- **(ii.1)** *if system (3.1) has a unique equilibrium (x_0, y_0), then (x_0, y_0) is a stable focus or node, and (x_0, y_0) attracts the set $\mathbb{R}^2_+$ under the flow of system (3.1).*
- **(ii.2)** *if system (3.1) has two equilibria (x_0^1, y_0^1) and (x_0^2, y_0^2), then the point at which $\psi_1(x) = \psi_2(x)$ holds is a saddle–node, the other point is a stable focus or node.*
- **(ii.3)** *if system (3.1) has three equilibria (x_0^i, y_0^i), $i = 1, 2, 3$, satisfying $x_0^1 < x_0^2 < x_0^3$, then (x_0^1, y_0^1) and (x_0^3, y_0^3) are a stable focus or node, and (x_0^2, y_0^2) is a saddle.*

Proof. Under the condition $\psi_1'(x_+) \geq 0$, Lemmas 3.1 and 3.2 yield that $\psi(0) = -v/c < 0$, $\psi' = \psi_1'(x) - \psi_2'(x) > 0$ for $x > 0$. Then there is a unique equilibrium (x_0, y_0) for system (3.1) in $\mathbb{R}^2_+$. Note that this equilibrium satisfies $D(x_0, y_0) > 0$ and $T(x_0, y_0) \leq -\varepsilon < 0$. Then (x_0, y_0) is a stable focus for $(\varepsilon - \psi_1'(x_0))^2 + 4\varepsilon\psi_2'(x_0) < 0$ and is a stable node for $(\varepsilon - \psi_1'(x_0))^2 + 4\varepsilon\psi_2'(x_0) \geq 0$. Assume that ψ_1 satisfies $\psi_1'(x_+) \geq 0$. By Lemma 3.1 we have that

$$\frac{\partial}{\partial x}(y - \psi_1(x)) + \frac{\partial}{\partial y}(\varepsilon(\psi_2(x) - y)) = -(\varepsilon + \psi_1'(x)) \leq -\varepsilon, \quad x \geq 0. \tag{4.5}$$

Hence, Bendixson's Theorem yields that system (3.1) has no periodic orbits in $\mathbb{R}^2_+$. Recall that (x_0, y_0) is a stable focus or node. Then (x_0, y_0) attracts the set $\mathbb{R}^2_+$ under the flow of system (3.1). Thus, the statements in **(i)** are proved.

If ψ_1 satisfies $-\varepsilon < \psi_1'(x_+) < 0$, then by similar method used in the proof for **(i)**, we obtain that system (3.1) has no periodic orbits in $\mathbb{R}^2_+$. As for the types of equilibria, we only give the proof for the case **(ii.2)**. Without loss of generality, assume that $\psi_1(x_0^1) = \psi_2(x_0^1)$ and $x_0^1 > x_0^2$. Then by Lemmas 3.1 and 3.2, we obtain that $T(x_0^i, y_0^i) < 0$, $\mathcal{D}(x_0^1, y_0^1) = 0$, $\mathcal{D}(x_0^2, y_0^2) > 0$ and $\varepsilon(\psi_1''(x_0) - \psi_2''(x_0)) < 0$. Hence, (x_0^2, y_0^2) is a stable focus or node, and by using [44, Theorem 7.1, p.114] (see also the proof in Theorem 5.2), we obtain that (x_0^1, y_0^1) is a saddle–node. Therefore, the proof is now complete. □

Remark 4.1. Whether an equilibrium is a focus or node, is determined by the sign of $\Delta(x_0, y_0) = (\varepsilon - \psi_1'(x_0))^2 + 4\varepsilon\psi_2'(x_0)$ (see [43,44]). More precisely, if $\Delta(x_0, y_0) = (\varepsilon - \psi_1'(x_0))^2 + 4\varepsilon\psi_2'(x_0) < 0$ (resp. ≥ 0), then it is a focus (resp. node). We also remark that for sufficiently large $\varepsilon = k_m/k_3 > |\psi_1'(x_+)|$, there are no periodic orbits in system (3.1).

5. Dynamics of the low degradation rate case

In this section, we consider the dynamics of the THTN model in the low degradation rate case, that is, the rate of mRNA degradation is low enough. Throughout this section, we always assume that $0 < \varepsilon \ll 1$ and v is independent of ε. Then system (3.1) is a standard slow–fast system of the form (2.1). For convenience, we write $\psi_1(x, \lambda)$ and $\psi_2(x, \lambda, v)$, instead of $\psi_1(x)$ and $\psi_2(x)$, where $\lambda = (a, b_1, b_2, c)$. Then system (3.1) can be written as

$$\begin{aligned} \frac{dx}{dt} &= x' = y - \psi_1(x, \lambda) := f(x, y, \lambda), \\ \frac{dy}{dt} &= y' = \varepsilon\,(\psi_2(x, \lambda, v) - y) := \varepsilon g(x, y, \lambda, v). \end{aligned} \tag{5.1}$$

By a time rescaling $s = \varepsilon t$, the slow system corresponding to system (5.1) is in the form

$$\begin{aligned} \varepsilon\frac{dx}{ds} &= \varepsilon\dot{x} = y - \psi_1(x, \lambda), \\ \frac{dy}{ds} &= \dot{y} = \psi_2(x, \lambda, v) - y. \end{aligned} \tag{5.2}$$

Let the set $\mathcal{C}_0$ be defined by $\mathcal{C}_0 = \{(x, y) \in \mathbb{R} \times \mathbb{R} : y = \psi_1(x, \lambda)\}$. Throughout this section we always assume that ψ_1 satisfies $\psi_1'(x_+) < 0$ for suitable parameters λ and v. Then the set $\mathcal{C}_0$ is S-shaped. Due to Lemma 3.1, all points in the set $\mathcal{C}_0$, except $(x_i, y_i) := (x_i, \psi_1(x_i))$, $i = m, M$, are normally hyperbolic. We now assume that the parameter ε is sufficiently small. Then Fenichel theory [22] is applicable, and normally hyperbolic invariant manifolds persist near the critical manifold for nonzero ε. The reduced system (see (2.4)) on $L^1 \cup M \cup R^1$ is governed by

$$\frac{\partial\psi_1}{\partial x}(x, \lambda)\frac{dx}{ds} = \psi_2(x, \lambda, v) - \psi_1(x, \lambda). \tag{5.3}$$

In the following, we investigate the dynamics of the THTN model in the low degradation rate case by employing geometric singular perturbation theory.

5.1. Local dynamics of canard points

We start by studying the local dynamics of canard points. Assume that for $\lambda = \lambda^0$ and $v = v^0$, either (x_m, y_m) or (x_M, y_M) is an equilibrium of the slow–fast system (5.1). Then at this point (x_i, y_i), $i = m$ or M, we have that $f(x_i, y_i, \lambda^0) = 0$ and $g(x_i, y_i, \lambda^0, v^0) = 0$. By Lemma 3.1 the function f satisfies

$$\frac{\partial f}{\partial x}(x_i, y_i, \lambda^0) = -\frac{\partial\psi_1}{\partial x}(x_i, \lambda^0) = 0.$$

Then the critical manifold $\mathcal{C}_0$ loses hyperbolicity at (x_i, y_i) and (x_i, y_i) is a contact point. By Lemmas 3.1 and 3.2, the slow–fast system (5.1) satisfies the nondegeneracy conditions:

$$\begin{aligned} &\frac{\partial^2 f}{\partial x^2}(x_i, y_i, \lambda^0) = -\frac{\partial^2\psi_1}{\partial x^2}(x_i, \lambda^0) \neq 0, \qquad \frac{\partial f}{\partial y}(x_i, y_i, \lambda^0) = 1, \\ &\frac{\partial g}{\partial x}(x_i, y_i, \lambda^0, v^0) = \frac{\partial\psi_2}{\partial x}(x_i, \lambda^0, v^0) < 0, \\ &\frac{\partial g}{\partial v}(x_i, y_i, \lambda^0, v^0) = \frac{1}{c^0 + (x_i - \phi(x_i))^2} > 0, \end{aligned}$$

where $\frac{\partial^2\psi_1}{\partial x^2}(x_i, \lambda^0) < 0$ for $i = m$ and $\frac{\partial^2\psi_1}{\partial x^2}(x_i, \lambda^0) > 0$ for $i = M$. Then by (3.2), (3.3) and (3.4) in [18, p. 303], the above

nondegeneracy conditions insure that the contact point (x_i, y_i) is a canard point of the slow–fast system (5.1).

We next consider the normal forms of system (5.1) near the canard points (x_i, y_i), $i = m, M$.

Lemma 5.1. *Assume that for $\lambda = \lambda^0$ and $v = v^0$, either (x_m, y_m) or (x_M, y_M) is an equilibrium of the slow–fast system (5.1). Then for a fixed $\lambda = \lambda^0$, the slow–fast system (5.1) near (x_m, y_m) and (x_M, y_M) can be changed into*

$$\begin{aligned} x' &= -y + x^2\Phi_1(x),\\ y' &= \varepsilon\left(x\Phi_2(x, v) - v + \frac{1}{D_1\psi_2(x_i, \lambda^0, v^0)}y\right), \end{aligned} \tag{5.4}$$

where Φ_j are defined by

$$\begin{aligned} \Phi_1(x) &= 1 + \frac{2}{\varphi_1''(0)}\widehat{\Phi}_1(-\frac{2}{\varphi_1''(0)}x),\\ \Phi_2(x, v) &= 1 + \frac{1}{D_1\varphi_2(0,0)}\widehat{\Phi}_2\left(-\frac{2}{\varphi_1''(0)}x,\right.\\ &\qquad \left.\frac{2D_1\varphi_2(0,0)(c^0 + (x_i - \phi(x_i))^2)}{\varphi_1''(0)}v\right), \end{aligned}$$

and the functions φ_j and $\widehat{\Phi}_j$ are in the form

$$\begin{aligned} \varphi_1(x) &= \psi_1(x + x_i, \lambda^0) - y_i,\\ \varphi_2(x, v) &= \psi_2(x + x_i, \lambda^0, v + v^0) - y_i,\\ \widehat{\Phi}_1(x) &= \int_0^1\int_0^1 \alpha\varphi_1''(\alpha\beta x)d\alpha d\beta - \frac{1}{2}\varphi_1''(0),\\ \widehat{\Phi}_2(x, v) &= x\int_0^1\int_0^1 \alpha D_{11}\varphi_2(\alpha\beta x, 0)d\alpha d\beta\\ &\quad + v\int_0^1\int_0^1 D_{12}\varphi_2(\alpha x, \beta v)d\alpha d\beta. \end{aligned} \tag{5.5}$$

Here, $D_{ij} = D_j \circ D_i$ and each D_j denotes the partial derivative with respect to the jth variable.

Proof. Assume that (x_i, y_i), $i = m$ or M, is an equilibrium of system (5.1) with $\lambda = \lambda^0$ and $v = v^0$. Let $\lambda = \lambda^0$ be fixed. Then by a translation transformation $\mathcal{T}_1$ of the form

$$\mathcal{T}_1 : (x, y, v) \to (x + x_i, y + y_i, v + v^0), \tag{5.6}$$

system (5.1) is transformed into the form

$$\begin{aligned} x' &= y - \varphi_1(x),\\ y' &= \varepsilon\left(\varphi_2(x, v) - y\right), \end{aligned} \tag{5.7}$$

where φ_i are defined by (5.5) satisfying $\varphi_1(0) = 0$, $\varphi_1'(0) = 0$ and $\varphi_2(0, 0) = 0$. Thus the function φ_1 can be written as the form

$$\varphi_1(x) = x\int_0^1 \varphi_1'(\alpha x)d\alpha = x^2\int_0^1\int_0^1 \alpha\varphi_1''(\alpha\beta x)d\alpha d\beta,$$

which implies

$$\varphi_1(x) = x^2\left(\frac{1}{2}\varphi_1''(0) + \widehat{\Phi}_1(x)\right).$$

Similarly, we have

$$\begin{aligned} \varphi_2(x, v) &= \varphi_2(x, v) - \varphi_2(0, v) + \varphi_2(0, v)\\ &= x\int_0^1 D_1\varphi_2(\alpha x, v)d\alpha + \frac{v}{c^0 + (x_i - \phi(x_i))^2}\\ &= x\left(D_1\varphi_2(0,0) + x\int_0^1\int_0^1 \alpha D_{11}\varphi_2(\alpha\beta x, 0)d\alpha d\beta\right.\\ &\quad \left. + v\int_0^1\int_0^1 D_{12}\varphi_2(\alpha x, \beta v)d\alpha d\beta\right)\\ &\quad + \frac{v}{c^0 + (x_i - \phi(x_i))^2}\\ &= x\left(D_1\varphi_2(0,0) + \widehat{\Phi}_2(x, v)\right) + \frac{v}{c^0 + (x_i - \phi(x_i))^2}. \end{aligned}$$

By taking a coordinate transformation $\mathcal{T}_2$ of the form

$$\begin{aligned} \mathcal{T}_2 : (x, y, v, \varepsilon) \to &\left(-\frac{2}{\varphi_1''(0)}x,\ \frac{2}{\varphi_1''(0)}y,\right.\\ &\left.\frac{2D_1\varphi_2(0,0)(c^0 + (x_i - \phi(x_i))^2)}{\varphi_1''(0)}v,\ -\frac{1}{D_1\varphi_2(0,0)}\varepsilon\right), \end{aligned} \tag{5.8}$$

system (5.7) is changed into the form (5.4). Therefore, the proof is now complete. □

Next we define several constants, which play important roles in the analysis of the dynamics near the canard points. Similarly to the formulas (3.12) and (3.13) in [19], let

$$\begin{aligned} &\kappa_{i,1} = \frac{d\Phi_1}{dx}(0), \quad \kappa_{i,2} = \frac{\partial\Phi_2}{\partial x}(0,0), \quad \kappa_{i,3} = \frac{1}{D_1\psi_2(x_i, \lambda^0, v^0)},\\ &i = m,\ M, \end{aligned}$$

and define A_i by

$$A_i = 3\kappa_{i,1} - 2\kappa_{i,2} - 2\kappa_{i,3}, \quad i = m,\ M.$$

Here the key constants A_i determine the nondegeneracy conditions for the Hopf bifurcations near the canard points (x_i, y_i) and are important for the analysis of canard explosions (see [19,20]). By a direct computation we obtain

$$\begin{aligned} \kappa_{i,1} &= -\frac{2D_{111}\psi_1(x_i, \lambda^0)}{3(D_{11}\psi_1(x_i, \lambda^0))^2},\\ \kappa_{i,2} &= -\frac{D_{11}\psi_2(x_i, \lambda^0, v^0)}{D_{11}\psi_1(x_i, \lambda^0)D_1\psi_2(x_i, \lambda^0, v^0)}, \quad \kappa_{i,3} = \frac{1}{D_1\psi_2(x_i, \lambda^0, v^0)},\\ A_i &= -\frac{2D_{111}\psi_1(x_i, \lambda^0)}{(D_{11}\psi_1(x_i, \lambda^0))^2} + \frac{2D_{11}\psi_2(x_i, \lambda^0, v^0)}{D_{11}\psi_1(x_i, \lambda^0)D_1\psi_2(x_i, \lambda^0, v^0)}\\ &\quad - \frac{2}{D_1\psi_2(x_i, \lambda^0, v^0)}. \end{aligned} \tag{5.9}$$

Compared the above notations to the corresponding ones in [18], the functions h_j in [18, system (3.6), p.304] are in the form

$$\begin{aligned} &h_1 = 1, \quad h_2 = \Phi_1, \quad h_3 = 0, \quad h_4 = \Phi_2, \quad h_5 = 1,\\ &h_6 = \frac{1}{D_1\psi_2(x_i, \lambda^0, v^0)}, \end{aligned}$$

and the constants a_j introduced in [18, p. 305] are in the form

$$a_1 = a_2 = 0, \quad a_3 = \kappa_{i,1}, \quad a_4 = \kappa_{i,2}, \quad a_5 = \kappa_{i,3}.$$

Since the constants A_i satisfy

$$\begin{aligned} &-\frac{1}{2}(D_{11}\psi_1(x_i, \lambda^0))^2 \cdot D_1\psi_2(x_i, \lambda^0, v^0) \cdot A_i\\ &= D_{111}\psi_1(x_i, \lambda^0) \cdot D_1\psi_2(x_i, \lambda^0, v^0) - D_{11}\psi_1(x_i, \lambda^0)\\ &\quad \cdot D_{11}\psi_2(x_i, \lambda^0, v^0) + (D_{11}\psi_1(x_i, \lambda^0))^2, \end{aligned}$$

by a direct computation we have that three different cases $A_i < 0$, $A_i > 0$ and $A_i = 0$ can appear under some suitable conditions. We follow [19] and analyze the canard explosion in (5.1). Thus, we assume that $A_i \neq 0$ for $i = m, M$. This implies that two Hopf bifurcations near (x_i, y_i) are both nondegenerate (see **(iv)** of Theorem 5.1). The cases $A_i = 0$ will be studied in the future.

For sufficiently small $\varepsilon > 0$, one can see that the manifolds L^1, M and R^1 perturb smoothly to locally invariant manifolds L^1_ε, M_ε and R^1_ε, respectively. Assume that (x_m, y_m) (resp. (x_M, y_M)) is a canard point. Let Σ_m (resp. Σ_M) be the cross-section of the curve M at the point $(x_m^0, \psi_1(x_m^0))$ (resp. $(x_M^0, \psi_1(x_M^0))$ along the x-direction, where x_m^0 (resp. x_M^0) satisfies that $x_m^0 - x_m$ (resp.

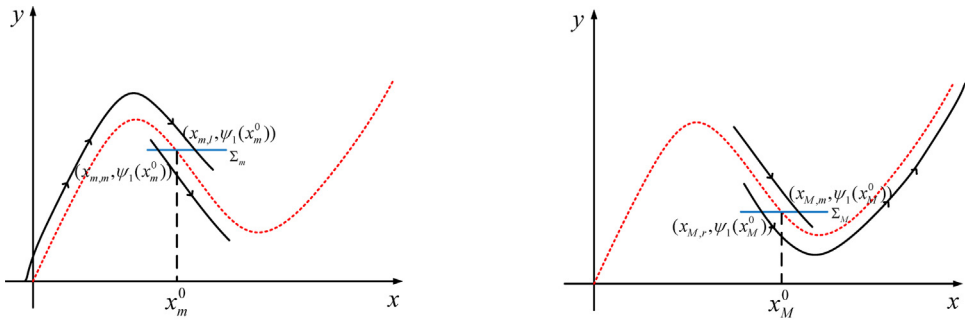

Fig. 3. Dynamics of the slow–fast system (5.1) near the canard points (x_m, y_m) and (x_M, y_M). The black curves are the orbits of system (5.1). The dashed red curves indicate the graph of function ψ_1.

$x_M - x_M^0$) is positive and sufficiently small. Let the manifold L_ε^1 (resp. R_ε^1) and M_ε extend in the neighborhood of this canard point. Assume that they respectively intersect with the section Σ_m (resp. Σ_M) at points $(x_{m,l}, \psi_1(x_m^0))$ and $(x_{m,m}, \psi_1(x_m^0))$ (resp. $(x_{M,m}, \psi_1(x_M^0))$ and $(x_{M,r}, \psi_1(x_M^0))$). See Fig. 3. We have the following results.

Lemma 5.2. *Assume that for $\lambda = \lambda^0$ and $v = v^0$, the slow–fast system (5.1) has an equilibrium at either (x_m, y_m) or (x_M, y_M) for $x \geq 0$. Then for sufficiently small $\varepsilon > 0$, there exist two smooth functions v_i^c, $i = m, M$, defined by*

$$v_i^c(\varepsilon) = v^0 + \mathcal{K}_i\varepsilon + O(\varepsilon^{3/2}), \quad i = m, M, \tag{5.10}$$

such that the slow–fast system (5.1) with $\lambda = \lambda^0$ has $x_{m,l} = x_{m,m}$ for $i = m$ and $x_{M,m} = x_{M,r}$ for $i = M$ if and only if $v = v_i^c(\varepsilon)$, where the constants $\mathcal{K}_i$ are defined by

$$\mathcal{K}_i = (\kappa_{i,3} + \frac{A_i}{4}) \cdot \frac{(D_1\psi_2(x_i, \lambda^0, v^0))^2(c^0 + (x_i - \phi(x_i))^2)}{D_{11}\psi_1(x_i, \lambda^0)}, \quad i = m, M. \tag{5.11}$$

Furthermore, if (x_m, y_m) is a canard point, then $x_{m,l} > x_{m,m}$ for $0 < v - v_m^c(\varepsilon) \ll 1$ and $x_{m,l} < x_{m,m}$ for $0 < v_m^c(\varepsilon) - v \ll 1$. If (x_M, y_M) is a canard point, then $x_{M,m} > x_{M,r}$ for $0 < v_M^c(\varepsilon) - v \ll 1$ and $x_{M,m} < x_{M,r}$ for $0 < v - v_M^c(\varepsilon) \ll 1$.

Proof. We only give the proof for the case (x_m, y_m). Under the transformation $\mathcal{T}_2 \circ \mathcal{T}_1$, we assume that the points $(x_{m,l}, \psi_1(x_m^0))$ and $(x_{m,m}, \psi_1(x_m^0))$ are changed to the points $(w_{m,l}, z_m)$ and $(w_{m,m}, z_m)$, respectively. Recall that the transformations $\mathcal{T}_j$, $j = 1, 2$, are given by (5.6) and (5.8), and $\varphi_1''(0) = D_{11}\psi_1(x_m, \lambda^0, v^0) < 0$. Then $x_{m,l} - x_{m,m}$ and $w_{m,l} - w_{m,m}$ have the same sign. To finish the proof for this lemma, we consider the normal form (5.4) of system (5.1) near (x_m, y_m). By [18, Theorem 3.1], there exists a smooth function $\widehat{v}_m^c(\cdot)$ defined by

$$\widehat{v}_m^c(\varepsilon) = -\frac{4\kappa_{m,3} + A_m}{8}\varepsilon + O(\varepsilon^{3/2})$$

such that system (5.4) has $w_{m,l} = w_{m,m}$ if and only if $v = \widehat{v}_m^c(\varepsilon)$. Thus, by taking the variable transformation $\mathcal{T}_1^{-1} \circ \mathcal{T}_2^{-1}$, we obtain that (5.10) holds for $i = m$. Since the constant d_{λ_2} in [18, Formula (3.23)] is negative, the remaining statements hold. Thus, the proof is finished. □

5.2. Global dynamics of the slow–fast circadian oscillator system

In this section, we study the global dynamics of the slow–fast system (5.1). The discussion is divided into three different parts according to the number of equilibria.

5.2.1. One equilibrium

Assume that the slow–fast system (5.1) with $\lambda = \lambda^0$ and $v = v^0$ has exactly one equilibrium (x_0, y_0) in the set $x \geq 0$. Then all types of the intersection point sequences are L^1, L^0, M, R^0 and R^1. See Figs. 2(a)–2(e).

If the unique equilibrium (x_0, y_0) is of type M, then (x_i, y_i) are both jump points. Let x_l (resp. x_r) be the value such that $\psi_1(x_l, \lambda^0) = y_M$ (resp. $\psi_1(x_r, \lambda^0) = y_m$) and $(x_l, y_M) \in L$ (resp. $(x_r, y_m) \in R$). We define a singular relaxation cycle Γ_r. See Fig. 4(a). This cycle Γ_r consists of four branches, among which two branches are the critical fibers of the layer equation joining (x_m, y_m) to (x_r, y_m) and (x_M, y_M) to (x_l, y_M), another two branches are the parts of the critical manifolds joining (x_l, y_M) to (x_m, y_m) and (x_r, y_m) to (x_M, y_M).

If the unique equilibrium (x_0, y_0) is of type L^0 or type R^0, then (x_m, y_m) or (x_M, y_M) is a canard point. As a preparation, we next begin with the construction of canard slow–fast cycles. See Figs. 4(b) and 4(c). For a positive constant θ with $0 < \theta < y_m - y_M$, let the constants x_j^m, $j = l, m, r$, with $0 < x_l^m(\theta) < x_m < x_m^m(\theta) < x_M < x_r^m(\theta)$, denote the roots of equation $\psi_1(x, \lambda^0) = y_m - \theta$. We define the canard slow–fast cycles $\Gamma_m(\theta)$, $0 \leq \theta \leq 2(y_m - y_M)$, for the canard point (x_m, y_m) as follows. For $0 \leq \theta \leq y_m - y_M$,

$$\begin{aligned}\Gamma_m(\theta) := &\left\{(x, \psi_1(x, \lambda^0)) : x \in [x_l^m(\theta), x_m^m(\theta)]\right\} \\ &\cup \left\{(x, y_m - \theta) : x \in [x_l^m(\theta), x_m^m(\theta)]\right\},\end{aligned}$$

and for $y_m - y_M \leq \theta \leq 2(y_m - y_M)$,

$$\begin{aligned}\Gamma_m(\theta) := &\left\{(x, \psi_1(x, \lambda^0)) : x \in [x_l, x_m^m(2(y_m - y_M) - \theta)]\right\} \\ &\cup \left\{(x, 2y_M + \theta - y_m) : x \in [x_m^m(2(y_m - y_M) - \theta), \right. \\ &\quad \left. x_r^m(2(y_m - y_M) - \theta)]\right\} \\ &\cup \left\{(x, \psi_1(x, \lambda^0)) : x \in [x_M, x_r^m(2(y_m - y_M) - \theta)]\right\} \\ &\cup \{(x, y_M) : x \in [x_l, x_M]\}.\end{aligned}$$

Similarly, we can define the family of slow–fast cycles $\Gamma_M(\cdot)$ for the canard point (x_M, y_M), the detail is omitted. Then we have the following statements.

Theorem 5.1. *Assume that for $\lambda = \lambda^0$ and $v = v^0$, the slow–fast system (5.1) has a unique equilibrium (x_0, y_0) in the set $x \geq 0$. Then for $\lambda = \lambda^0$, $v = v^0$ and sufficiently small $\varepsilon > 0$, the following statements hold:*

- **(i)** *if the equilibrium (x_0, y_0) is in the set L^1 (resp. R^1), then system (5.1) has no periodic orbits in the set $\mathbb{R}_+^2$, and (x_0, y_0) is a stable node and attracts the set $\mathbb{R}_+^2$ under the flow of system (5.1).*
- **(ii)** *if the equilibrium (x_0, y_0) is in the set M, then for sufficiently small $\varepsilon > 0$, the equilibrium (x_0, y_0) is an unstable node, and*

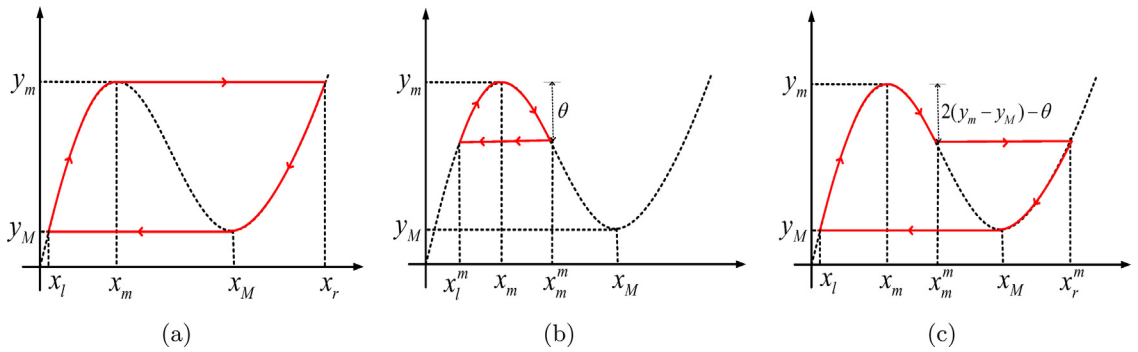

Fig. 4. Slow–fast cycles (the red curves) are constructed: 4(a) Singular relaxation cycle. 4(b) Canard slow–fast cycle without head. 4(c) Canard slow–fast cycle with head. (For interpretation of the references to color in this figure legend, the reader is referred to the web version of this article.)

there exists a unique limit cycle $\Gamma_{r,\varepsilon}$ in a small neighborhood of the slow–fast cycle Γ_r. Furthermore, the limit cycle $\Gamma_{r,\varepsilon}$ is locally asymptotically stable with the Floquet exponent bounded above by $-C/\varepsilon$ for some $C > 0$, and $\Gamma_{r,\varepsilon} \to \Gamma_r$ as $\varepsilon \to 0$ in the sense of Hausdorff distance.

(iii) *if the equilibrium (x_0, y_0) is in the set L^0 (resp. R^0), then (x_0, y_0) is a stable focus.*
Further, for the intersection point sequences L^0 and R^0, let $\lambda = \lambda^0$ be fixed and the parameter v vary. Then for sufficiently small $\varepsilon > 0$, the following assertions hold:

(iv) *there exists a $V_0 > 0$ such that for each v with $|v - v^0| < V_0$, system (5.1) possesses a unique equilibrium near (x_m, y_m) (resp. (x_M, y_M)) in the set $x \geq 0$, which converges to (x_m, y_m) (resp. (x_M, y_M)) as $(v, \varepsilon) \to (v^0, 0)$. Moreover, there exist two Hopf bifurcation curves v_i^H defined by*

$$v_i^H(\varepsilon) = v^0 + \frac{\kappa_{i,3}(D_1\psi_2(x_i, \lambda^0, v^0))^2(c^0 + (x_i - \phi(x_i))^2)}{D_{11}\psi_1(x_i, \lambda^0)}\varepsilon + O(\varepsilon^{3/2}), \quad i = m, M, \tag{5.12}$$

such that this equilibrium is stable for $v < v_m^H(\varepsilon)$ (resp. $v > v_M^H(\varepsilon)$) and is unstable for $v > v_m^H(\varepsilon)$ (resp. $v < v_M^H(\varepsilon)$). These Hopf bifurcations are nondegenerate if the constants A_i given by (5.9) satisfy $A_i \neq 0$, $i = m, M$, and are supercritical for $A_m < 0$ (resp. $A_M > 0$) and are subcritical for $A_m > 0$ (resp. $A_M < 0$).

(v) *fix some $\gamma \in (0, 1)$ and assume that A_i defined by (5.9) satisfy $A_i \neq 0$. Then for each $i = m, M$, there exists a smooth family of periodic orbits*

$$(\theta, \varepsilon) \to (v_i(\theta, \varepsilon),\ \Gamma_i(\theta, \varepsilon)), \quad \varepsilon \in (0, \varepsilon_0), \quad \theta \in (0, 2(y_m - y_M)),$$

such that $\Gamma_i(\theta, \varepsilon) \to \Gamma_i(\theta)$ as $\varepsilon \to 0$. More precisely, the periodic orbit $\Gamma_i(\theta, \varepsilon)$ is $O(\varepsilon^\gamma)$-close to the canard point (x_i, y_i) for each $\theta \in \left(0, \left(-D_1\psi_2(x_i, \lambda^0, v^0)\varepsilon\right)^\gamma\right)$, a relaxation oscillation for each $\theta \in \left(2y_m - \left(-D_1\psi_2(x_i, \lambda^0, v^0)\varepsilon\right)^\gamma, 2y_m\right)$, and a canard cycle for $v = v_i(\theta, \varepsilon)$ and each $\theta \in \left[\left(-D_1\psi_2(x_i, \lambda^0, v^0)\varepsilon\right)^\gamma, 2y_m - \left(-D_1\psi_2(x_i, \lambda^0, v^0)\varepsilon\right)^\gamma\right]$, where $v_i(\theta, \varepsilon)$ satisfies

$$|v_i(\theta, \varepsilon) - v_i^c(\varepsilon)| \leq \frac{D_{11}\psi_1(x_i, \lambda^0)}{2D_1\psi_2(x_i, \lambda_0, v^0)(c^0 + (x_i - \phi(x_i))^2)} \times e^{-\left(-D_1\psi_2(x_i, \lambda^0, v^0)\varepsilon\right)^{\gamma-1}}, \tag{5.13}$$

and v_i^c is in the form (5.10).

(vi) *if $(x_0, y_0) = (x_m, y_m)$ is a canard point, then for $A_m > 0$ and some v with $v_m^c(\varepsilon) < v < v_m^H(\varepsilon)$, there are two coexistent periodic orbits surrounding the equilibrium (x_m, y_m), where the inner one is unstable and the outer one is stable. If $(x_0, y_0) = (x_M, y_M)$ is a canard point, then for $A_M < 0$ and some v with $v_M^c(\varepsilon) < v < v_M^H(\varepsilon)$, there are two coexistent periodic orbits surrounding the equilibrium (x_M, y_M), where the inner one is stable and the outer one is unstable.*

Proof. We omitted the proofs for the types of the equilibria, which can be obtained by a standard analysis. The dynamics of the layer equations and the reduced systems are shown in Fig. 2.

To prove **(i)**, we only consider the case $(x_0, y_0) \in L^1$, as the other one can be similarly proved. Note that the manifold L^1 is normally hyperbolic and transversally intersects with x-axis. Then by [22, Theorem 9.1], the manifold L^1 perturbs smoothly to locally invariant manifolds L_ε^1 which connects (x_0, y_0) to a point at x-axis and transversally intersects with x-axis. Then no periodic orbits surround (x_0, y_0). This together with Lemma 4.1 yields the attraction of (x_0, y_0). Thus, **(i)** is obtained.

To prove **(ii)**, assume that for $\lambda = \lambda^0$ and $v = v^0$ type M appears. By Lemmas 3.1 and 3.2, system (5.3) satisfies $\dot{y} > 0$ for $0 < x < x_m$ and $\dot{x} < 0$ for $x > x_M$, and the stability of the critical manifold $\mathcal{C}_0$ changes at points (x_i, y_i) for the layer equation. The statements on the limit cycle $\Gamma_{r,\varepsilon}$ can be proved by applying [19, Theorem 2.1, p. 318] and [22, Theorem 9.1]. Thus, **(ii)** is obtained.

To prove **(iv)**, we recall that the existence and location of equilibria for the slow–fast system (5.1) are independent of ε. Then the first statement holds. By [19, Formula (3.15), p.326], for each $i = m, M$, the Hopf bifurcation curve $\widehat{V}_i^H$ for the normal form (5.4) is in the form

$$\widehat{V}_i^H(\varepsilon) = -\frac{\kappa_{i3}}{2}\varepsilon + O(\varepsilon^{3/2}) = -\frac{1}{2D_1\psi_2(x_i, \lambda^0, v^0)}\varepsilon + O(\varepsilon^{3/2}).$$

Thus by the transformation $\mathcal{T}_1^{-1} \circ \mathcal{T}_2^{-1}$, we obtain the Hopf bifurcation curve given by (5.12). Note that for canard point (x_m, y_m) (resp. (x_M, y_M)), the transformation $\mathcal{T}_2$ does not change (resp. changes) the sign of v. Then from [19, Theorem 3.1] it follows that the remaining statements in **(iv)** hold.

To prove **(v)**, we first consider the normal form (5.4) of the slow–fast system (5.1) near the canard points (x_i, y_i). Then by applying Theorems 3.3 and 3.5 in [19], we can prove **(v)** by the similar method used in the proof for **(iv)**.

To prove **(vi)**, we only consider the case $(x_0, y_0) = (x_m, y_m)$, as the other one can be similarly proved. Assume that $A_m > 0$. Then by $D_{11}\psi_1(x_m, \lambda^0) < 0$, (5.10) and (5.12), we have that

$$v_m^c(\varepsilon) < v_m^H(\varepsilon), \qquad v_m^H(\varepsilon) - v_m^c(\varepsilon) = O(\varepsilon)$$

for sufficiently small $\varepsilon > 0$, where $v_m^c(\varepsilon)$ and $v_m^H(\varepsilon)$ control the Hopf bifurcation and the intersection of slow manifolds near (x_m, y_m), respectively. Let a sufficiently small $\varepsilon > 0$ be fixed and vary v from $v_m^c(\varepsilon)$ to $v_m^H(\varepsilon)$. When v is in an exponentially small neighborhood of $v_m^c(\varepsilon)$ and satisfies $v_m^c(\varepsilon) < v < v_m^H(\varepsilon)$, by Lemma 5.2 and **(v)** in this theorem we have $x_{m,l} > x_{m,m}$ and a canard cycle with head appears. By the bifurcation diagram in

[19, Figure 7 (b), p. 328], the amplitude of this limit cycle increases as v increases and this persistent limit cycle is a relaxation oscillation or a stable canard cycle with head for each v in a small neighborhood of $v_m^H(\varepsilon)$. Then we obtain the outer limit cycle. By **(iv)** in this theorem, the Hopf bifurcation is subcritical for $A_m > 0$. Then there exists a sufficiently small $\tilde{V}_0 > 0$ such that for each v with $0 < v_m^H(\varepsilon) - v < \tilde{V}_0$, an unstable limit cycle arises from the subcritical Hopf bifurcation and coexists with the obtained large amplitude limit cycle. Thus, two coexistent periodic orbits are obtained and **(vi)** is proved. This finishes the proof. □

5.2.2. Two equilibria

Assume that the slow–fast system (5.1) has precisely two equilibria in the set $x \geq 0$ for some $\lambda = \lambda^0$ and $v = v^0$. Then all possible intersection point sequences are as follows: L^0M, L^1M, MM, MR^0 and MR^1. See Figs. 2(f)–2(j).

We first show that one of equilibria in M is a saddle–node and the slow–fast system (5.1) undergoes saddle–node bifurcation [45, Section 3.4] as the parameter v varies.

Theorem 5.2. *Assume that for $\lambda = \lambda^0$ and $v = v^0$, the slow–fast system (5.1) has precisely two equilibria in the half plane $x \geq 0$. Then the following statements hold:*

- **(i)** *for sufficiently small $\varepsilon > 0$, system (5.1) has a saddle–node point $(x_0, y_0) \in M$, at which system (5.1) satisfies $D_1\psi_1(x_0, \lambda^0) = D_1\psi_2(x_0, \lambda^0, v^0)$ and $D_{11}\psi_1(x_0, \lambda^0) \neq D_{11}\psi_2(x_0, \lambda^0, v^0)$.*
- **(ii)** *let $\lambda = \lambda^0$ be fixed and the parameter v vary. Then system (5.1) undergoes a saddle–node bifurcation, more precisely, if $\psi_1(x, \lambda^0) \leq \psi_2(x, \lambda^0, v^0)$ (resp. $\psi_1(x, \lambda^0) \geq \psi_2(x, \lambda^0, v^0)$) near $x = x_0$, then for small $|v - v^0|$, system (5.1) has no equilibria near (x_0, y_0) for $v > v^0$ (resp. $v < v^0$), and system (5.1) has two equilibria (x_0^1, y_0^1) and (x_0^2, y_0^2) satisfying $x_0^1 < x_0^2$ near (x_0, y_0) for $v < v^0$ (resp. $v > v^0$), where (x_0^1, y_0^1) is an unstable node (resp. a saddle) and (x_0^1, y_0^1) is a saddle (resp. an unstable node).*

Proof. Assume that system (5.1) has precisely two equilibria in the set $x \geq 0$ for $\lambda = \lambda^0$ and $v = v^0$, then by Lemmas 3.2 and 3.3, there exists precisely one equilibrium (x_0, y_0) in M, which is a tangent point between functions ψ_1 and ψ_2, that is, $D_1\psi_1(x_0, \lambda^0) = D_1\psi_2(x_0, \lambda^0, v^0)$. Then for sufficiently small $\varepsilon > 0$, the functions $\mathcal{D}(\cdot, \cdot)$, $T(\cdot, \cdot)$ and $\Delta(\cdot, \cdot)$ defined by (4.3) and (4.4) satisfy

$$\mathcal{D}(x_0, y_0) = 0, \quad T(x_0, y_0) > 0, \quad \Delta(x_0, y_0) > 0,$$

and the eigenvalues of the Jacobian matrix $\mathcal{J}(x_0, y_0)$ are $\mu_1 = -\varepsilon - D_1\psi_1(x_0, \lambda^0) > 0$ and $\mu_2 = 0$. By a change

$$(x, y) \to (\bar{x} + \bar{y} + x_0, D_1\psi_1(x_0, \lambda^0)\bar{x} - \varepsilon\bar{y} + y_0),$$

and then dropping the bars over the variables, we can change system (5.1) into

$$\begin{aligned} \frac{dx}{dt} &= X_2(x + y), \\ \frac{dy}{dt} &= \mu_1 y + Y_2(x + y), \end{aligned} \tag{5.14}$$

where X_2 and Y_2 are given by

$$\begin{aligned} X_2(x) &= \frac{\varepsilon}{D_1\psi_1(x_0, \lambda^0) + \varepsilon} \left(\psi_2(x + x_0, \lambda^0, v^0) - \psi_1(x + x_0, \lambda^0)\right), \\ Y_2(x) &= -\frac{1}{D_1\psi_1(x_0, \lambda^0) + \varepsilon} \left(D_1\psi_1(x_0, \lambda^0)\psi_1(x + x_0, \lambda^0)\right. \\ &\quad \left. + \varepsilon\psi_2(x + x_0, \lambda^0, v^0)\right) \\ &\quad + D_1\psi_1(x_0, \lambda^0)x + y_0. \end{aligned}$$

Clearly, $X_2(0) = Y_2(0) = X_2'(0) = Y_2'(0) = 0$. Then by the Implicit Function Theorem, there exists a smooth function $y = y(x)$ with $y(0) = y'(0) = 0$ such that $\mu_1 y(x) + Y_2(x, y(x)) = 0$ in a neighborhood of $(0, 0)$. By a direct computation, for small $|x|$ the function $X_2(\cdot + y(\cdot))$ can be expanded as the form

$$X_2(x + y(x)) = K_2 x^2 + O(x^3),$$

where the coefficient K_2 is in the form

$$K_2 = \frac{\varepsilon \left(D_{11}\psi_2(x_0, \lambda^0, v^0) - D_{11}\psi_1(x_0, \lambda^0)\right)}{D_1\psi_1(x_0, \lambda^0) + \varepsilon}.$$

By Lemma 3.2 we have $K_2 \neq 0$. Thus, [43, Theorem 2.19, p.74] yields that the equilibrium $(x_0, y_0) \in M$ is a saddle–node. Then **(i)** holds.

To prove **(ii)**, we only consider the case that $\psi_1(x, \lambda^0) \leq \psi_2(x, \lambda^0, v^0)$ for small $|x - x_0|$, as the other case can be similarly discussed. Then we have

$$D_{11}\psi_2(x_0, \lambda^0, v^0) - D_{11}\psi_1(x_0, \lambda^0) > 0.$$

Consider (5.14) with v^0 replaced by $v + v^0$. By the center manifold theory [46, Section 1.3], the flow on the center manifold for an equivalent system of (5.14) is governed by

$$\begin{aligned} \frac{dx}{dt} &= \frac{\varepsilon}{D_1\psi_1(x_0, \lambda^0) + \varepsilon} \left(\left(\frac{1}{c^0 + (x_0 - \phi(x_0))^2} \right.\right. \\ &\quad \left. + D_{13}\psi_2(x_0, \lambda^0, v^0)x \right) v \\ &\quad \left. + \frac{1}{2} \left(D_{11}\psi_2(x_0, \lambda^0, v^0) - D_{11}\psi_1(x_0, \lambda^0)\right) x^2 \right) + O(|(x, v)|^3) \\ \frac{dv}{dt} &= 0. \end{aligned} \tag{5.15}$$

The proof for (5.15) is given in Appendix B. Since $D_1\psi_1(x_0, \lambda^0) < 0$, for sufficiently small ε system (5.15) has no equilibria near $x = 0$ for $v > 0$ and has two equilibria $x = x_1(v)$ and $x = x_2(v)$ with $x_1(v) < x_2(v)$ near $x = 0$ for $v < 0$, where $x = x_1(v)$ and $x = x_2(v)$ are an unstable node and a stable node, respectively. See Fig. 5. Then **(ii)** holds. Therefore, the proof is now complete. □

By the above theorem, we observe that the equilibrium of type M in the sequences L^1M, MR^1, L^0M and MR^0 is a saddle–node, so is one of the equilibria in the sequence MM. More properties of the slow–fast system (5.1) with two equilibria are given in the next results.

Theorem 5.3. *Assume that the slow–fast system (5.1) has precisely two equilibria in the set $x \geq 0$ for $\lambda = \lambda^0$ and $v = v^0$. Then for sufficiently small $\varepsilon > 0$, the following statements hold:*

- **(i)** *if the intersection point sequence is L^1M (resp. MR^1), then system (5.1) has a stable node (x_0^1, y_0^1) in L^1 (resp. R^1), a saddle–node (x_0^2, y_0^2) in M, no periodic orbits in the set $x \geq 0$ and infinitely many heteroclinic orbits joining (x_0^2, y_0^2) to (x_0^1, y_0^1). Further, all orbits starting from the first quadrant including its boundary, except a unique center manifold of (x_0^2, y_0^2), converge to the stable node (x_0^1, y_0^1) as time goes to infinity.*
- **(ii)** *if the intersection point sequence is MM, then system (5.1) has an unstable node $(x_0^1, y_0^1) \in M$, a saddle–node $(x_0^2, y_0^2) \in M$, and a unique heteroclinic orbit joining the unstable node to the saddle–node.*
- **(iii)** *if the intersection point sequence is L^0M (resp. MR^0), then system (5.1) has a stable focus (x_0^1, y_0^1) in L^0 (resp. R^0) and a saddle–node (x_0^2, y_0^2) in M. Let $\lambda = \lambda^0$ be fixed and the*

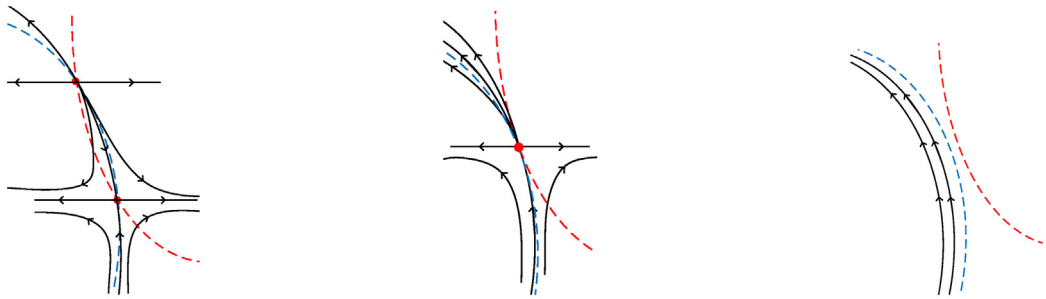

Fig. 5. Saddle–node bifurcation.

parameter v satisfy $|v - v^0| \ll 1$. Then system (5.1) has a homoclinic orbit, which closes to either a canard slow–fast cycle without head or a canard slow–fast cycle with head, if and only if $\kappa_{i,3}+A_i/4 < 0$ and $v = v_i^c(\varepsilon)$, where the functions v_i^c are defined by (5.10). Furthermore, if $\kappa_{i,3} + A_i/4 < 0$ and $0 < v - v_m^c(\varepsilon) \ll 1$ (resp. $0 < v_M^c(\varepsilon) - v \ll 1$), then either an unstable canard cycle with head or an unstable canard cycle without head bifurcates from this homoclinic orbit.

Throughout the proof for this theorem, we omit the proofs for the types of the equilibria. Dynamics of the cases L^1M, MM and L^0M are illustrated by Fig. 6.

Proof. To prove **(i)**, we only give the proof for type L^1M. Similarly to **(i)** of Theorem 5.1, system (5.1) with sufficiently small $\varepsilon > 0$ has no periodic orbits surrounding (x_0^1, y_0^1). Note that $dx/dt < 0$ along $y = \psi_2(x, \lambda^0)$ with $x > x_0^1$ and $x \neq x_0^2$. Then no periodic orbits exist in the first quadrant. By Theorem 5.2, we obtain that the saddle–node (x_0^2, y_0^2) possesses a unique center manifold approaching to it and infinitely many center manifolds leaving it. Hence, there are infinitely many orbits, which leave the saddle–node point (x_0^2, y_0^2), joining (x_0^2, y_0^2) to (x_0^1, y_0^1), and a unique orbit approaching to (x_0^2, y_0^2). Thus, the proof for **(i)** is finished by using Lemma 4.1.

To prove **(ii)**, assume that (x_0^1, y_0^1) and (x_0^2, y_0^2) are a transversal point and a tangent point of the functions ψ_1 and ψ_2, respectively. Without loss of generality, assume that $x_0^1 < x_0^2$ (see Fig. 6(b)). By Theorem 5.2, there is a unique center manifold on which the orbit approaches to (x_0^2, y_0^2) from the above and infinitely many orbits leaving (x_0^2, y_0^2). The existence and uniqueness of heteroclinic orbits are derived from the persistence of normally hyperbolic invariant manifolds. Thus, the proof for **(ii)** is finished.

To prove **(iii)**, we only consider type L^0M (see Fig. 6(c)). Let the notations be given as in Lemma 5.2. If $\kappa_{m,3} + A_m/4 < 0$ and $v = v_m^c(\varepsilon)$, then by $D_{11}\psi_1(x_m, \lambda^0) < 0$ and (5.10), we obtain that $v = v_m^c(\varepsilon) > 0$. This together with Theorem 5.2 yields that there are a saddle $(\widetilde{x}_0^2, \widetilde{y}_0^2)$ and an unstable node (x_0^3, y_0^3), which bifurcate from the saddle–node (x_0^2, y_0^2) and satisfy $x_0^1 < \widetilde{x}_0^2 < x_0^3$. By Lemma 5.2, we obtain a homoclinic orbit, which is homoclinic to the saddle $(\widetilde{x}_0^2, \widetilde{y}_0^2)$ and together with this saddle forms a small loop near a canard slow–fast cycle without head (see Fig. 7(a)) or a big loop near a canard slow–fast cycle with head (see Fig. 7(b)). If either $\kappa_{m,3} + A_m/4 > 0$ or $v \neq v_m^c(\varepsilon)$, then by Lemma 5.2 and Theorem 5.2, no homoclinic orbits exist in system (5.1) with sufficiently small ε. To prove the last statement, assume that $\kappa_{m,3} + A_m/4 < 0$ and $0 < v - v_m^c(\varepsilon) \ll 1$. Then by Lemma 5.2 we obtain that $x_{m,l} > x_{m,m}$. Note that the first order saddle quantity $T(\widetilde{x}_0^2, \widetilde{y}_0^2)$ of the saddle $(\widetilde{x}_0^2, \widetilde{y}_0^2)$ satisfies $T(\widetilde{x}_0^2, \widetilde{y}_0^2) > 0$ for sufficiently small ε. Then by [47, Theorem 3.3, p. 357], an unstable periodic orbit bifurcates from this homoclinic orbit. Furthermore, if the homoclinic orbit is small, then the perturbed periodic orbit is a canard cycle without head. If the homoclinic orbit is big, then it is a canard cycle with head. Thus, we obtain **(iii)**. This finishes the proof. □

5.2.3. Three equilibria

Assume that the slow–fast system (5.1) possesses three equilibria for some $\lambda = \lambda^0$ and $v = v^0$. Then all possible intersection point sequences are L^0MR^0, L^0MR^1, L^1MR^0, L^1MR^1, L^0MM, L^1MM, MMM, MMR^0 and MMR^1. See Figs. 2(k)–2(s). The main results for this case are summarized as follows.

Theorem 5.4. *Assume that the slow–fast system (5.1) has precisely three equilibria (x_0^i, y_0^i), $i = 1, 2, 3$, in the set $x \geq 0$ for $\lambda = \lambda^0$ and $v = v^0$, where $x_0^1 < x_0^2 < x_0^3$. Then for sufficiently small $\varepsilon > 0$, the following statements hold:*

- **(i)** *if the intersection point sequence is L^1MR^1, then $(x_0^1, y_0^1) \in L^1$ and $(x_0^3, y_0^3) \in R^1$ are stable nodes and $(x_0^2, y_0^2) \in M$ is a saddle, system (5.1) has no periodic orbits in the set $x \geq 0$, and two heteroclinic orbits joining (x_0^2, y_0^2) to (x_0^1, y_0^1) and (x_0^2, y_0^2) to (x_0^3, y_0^3), respectively. Furthermore, the set $\mathcal{A}$ defined as in Lemma 4.1 is divided into two disjoint sets Ω_1 and Ω_2 by the stable manifolds of (x_0^2, y_0^2), and all orbits starting from the interior of Ω_1 (resp. Ω_2) converge to (x_0^1, y_0^1) (resp. (x_0^3, y_0^3)) as time goes to infinity.*
- **(ii)** *if the intersection point sequence is MMM, then (x_0^1, y_0^1) and (x_0^3, y_0^3) are unstable nodes and (x_0^2, y_0^2) is a saddle, and a locally asymptotically stable relaxation oscillation $\Gamma_{r,\varepsilon}$ arising from the singular relaxation cycle Γ_r approaches to Γ_r in the sense of Hausdorff distance as $\varepsilon \to 0$, where the singular relaxation cycle Γ_r is constructed as in Fig. 4(a).*
- **(iii)** *if the intersection point sequence is L^1MM (resp. MMR^1), then $(x_0^1, y_0^1) \in L^1$ (resp. $(x_0^3, y_0^3) \in R^1$) is a stable node, $(x_0^2, y_0^2) \in M$ is a saddle and $(x_0^3, y_0^3) \in M$ (resp. $(x_0^1, y_0^1) \in M$) is an unstable node, and system (5.1) has no periodic orbits in the first quadrant, a heteroclinic orbit connecting (x_0^2, y_0^2) to (x_0^3, y_0^3) (resp. (x_0^1, y_0^1)), two heteroclinic orbits connecting (x_0^2, y_0^2) to (x_0^1, y_0^1) (resp. (x_0^3, y_0^3)) and infinitely many heteroclinic orbits connecting (x_0^3, y_0^3) to (x_0^1, y_0^1).*
- **(iv)** *if the intersection point sequence is L^0MM (resp. MMR^0), then $(x_0^1, y_0^1) \in L^0$ (resp. $(x_0^3, y_0^3) \in R^0$) is a stable focus, $(x_0^2, y_0^2) \in M$ is a saddle and $(x_0^3, y_0^3) \in M$ (resp. $(x_0^1, y_0^1) \in M$) is an unstable node, and system (5.1) has a heteroclinic orbit connecting (x_0^2, y_0^2) to (x_0^3, y_0^3) (resp. (x_0^1, y_0^1)). Further, let $\lambda = \lambda^0$ be fixed and the parameter v vary. Then for $(x_0^1, y_0^1) \in L^0$ (resp. $(x_0^3, y_0^3) \in R^0$), system (5.1) undergoes Hopf bifurcation and canard explosion in the ways as in Theorems 5.1 **(iv)** and **(v)**, respectively.*
- **(v)** *if the intersection point sequence is L^0MR^1 (resp. L^1MR^0), then $(x_0^1, y_0^1) \in L^0$ (resp. $(x_0^3, y_0^3) \in R^0$) is a stable focus, $(x_0^2, y_0^2) \in M$ is a saddle and $(x_0^3, y_0^3) \in R^1$ (resp. $(x_0^1, y_0^1) \in L^1$) is a*

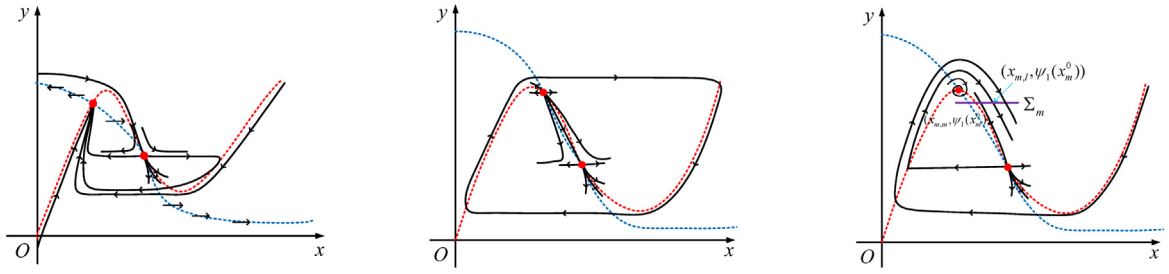

(a) L^1M (b) MM (c) L^0M

Fig. 6. Dynamics of the slow–fast system (5.1) with two equilibria in the set $x \geq 0$. The solid black curves are the orbits of system (5.1), the graphs of the functions ψ_1 and ψ_2 respectively indicate the dashed red and the dashed blue curves.

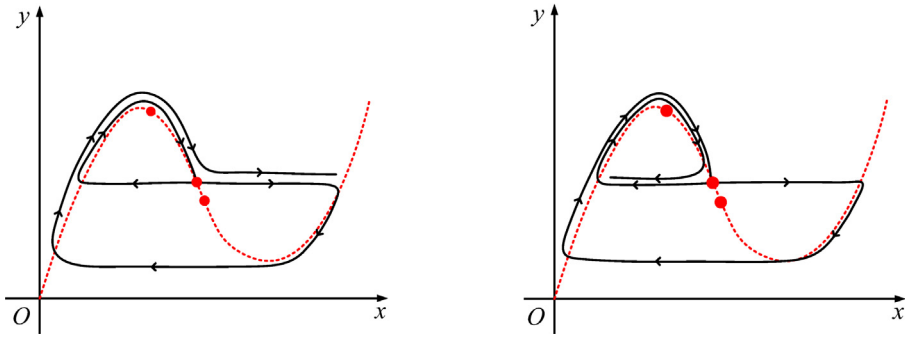

(a) Small homoclinic orbit. (b) Big homoclinic orbit.

Fig. 7. Two possible homoclinic orbits arise in type L^0M. The red dots are equilibria, the solid black curves are the orbits of system (5.1), and the graphs of the functions ψ_1 and ψ_2 respectively indicate the dashed red and the dashed blue curves.

stable node. Further, let $\lambda = \lambda^0$ be fixed and v vary. Then the following statements hold:

(v.1) *system (5.1) undergoes Hopf bifurcation according to Theorem 5.1***(iv)***.*

(v.2) *system (5.1) has no relaxation oscillations or canard cycles with head as v varies near v^0.*

(v.3) *there are two smooth functions v_i^c, $i = m, M$, having the expansions in (5.10) such that system (5.1) possesses a homoclinic orbit, which is homoclinic to a saddle in M and lies near a canard slow–fast cycle without head, if and only if $v = v_i^c(\varepsilon)$.*

(v.4) *if $0 < v - v_m^c(\varepsilon) \ll 1$ (resp. $0 < v_M^c(\varepsilon) - v \ll 1$), then an unstable canard cycle without head bifurcates from this homoclinic orbit. If $0 < v_m^c(\varepsilon) - v \ll 1$ (resp. $0 < v - v_M^c(\varepsilon) \ll 1$), then there exist no periodic orbits bifurcating from this homoclinic orbit.*

(vi) *if the intersection point sequence is L^0MR^0, then $(x_0^1, y_0^1) \in L^0$ is a stable focus, $(x_0^2, y_0^2) \in M$ is a saddle and $(x_0^3, y_0^3) \in R^0$ is a stable focus. Further, let $\lambda = \lambda^0$ be fixed and v vary. Then the following statements hold:*

(vi.1) *system (5.1) undergoes a Hopf bifurcation near (x_m, y_m) or (x_M, y_M) according to the way stated in Theorem 5.1***(iv)***, but not simultaneously.*

(vi.2) *there are two smooth functions v_i^c, $i = m, M$, defined by (5.10) such that system (5.1) has a homoclinic orbit, which is homoclinic to a saddle in M, if and only if $v = v_i^c(\varepsilon)$.*

(vi.3) *assume that the constants $\mathcal{K}_i$ defined by (5.11) satisfy $\mathcal{K}_m \neq \mathcal{K}_M$. Then for v satisfying $0 < v - v_m^c(\varepsilon) \ll 1$ (resp. $0 < v_M^c(\varepsilon) - v \ll 1$), there exists an unstable canard cycle bifurcating from the homoclinic orbit corresponding to $v = v_m^c(\varepsilon)$ (resp. $v = v_M^c(\varepsilon)$), and these two canard cycles cannot appear simultaneously. If v satisfies $0 < v_m^c(\varepsilon) - v \ll 1$ (resp. $0 < v - v_M^c(\varepsilon) \ll 1$), then there are no periodic orbits bifurcating from the homoclinic orbit corresponding to $v = v_m^c(\varepsilon)$ (resp. $v = v_M^c(\varepsilon)$).*

Proof. Here we also omitted the proofs for the types of the equilibria.

To prove **(i)**, we first consider the existence of periodic orbits. Similarly to Theorem 5.1**(i)**, no periodic orbits surround stable nodes (x_0^1, y_0^1) and (x_0^3, y_0^3). Since (x_i, y_i), $i = m, M$, are jump points, by [18, Theorem 2.1, p.290] we have that the stable manifolds of (x_0^2, y_0^2) extend to the boundary of the set $\mathcal{A}$. Hence, the stable manifolds of (x_0^2, y_0^2) cut $\mathcal{A}$ into two disjoint parts, and no periodic orbits surround (x_0^2, y_0^2). Thus, no periodic orbits exist. The invariant property of $\mathcal{A}$ yields the last statement. Thus, **(i)** is proved.

Similarly to Theorem 5.1**(ii)**, we can obtain **(ii)** in this theorem.

To prove **(iii)**, we only consider type L^1MM. Similarly to Theorem 5.1**(i)**, no periodic orbits surround (x_0^1, y_0^1). Note that the manifold M smoothly perturbs to locally invariant manifold M_ε, which connects (x_0^2, y_0^2) to (x_0^3, y_0^3). Then system (5.1) with sufficiently small ε has no periodic orbits in the first quadrant. Thus, **(iii)** is obtained.

To prove **(iv)**, for type L^0MM (resp. MMR^0), the slow manifold M_ε connects (x_0^2, y_0^2) to (x_0^3, y_0^3) (resp. (x_0^1, y_0^1)). Then the existence of the heteroclinic orbit is obtained. The assertions **(iv)** and **(v)** in Theorem 5.1 yield that the last statement holds. Thus, **(iv)** is proved.

To prove **(v)**, we only discuss type L^0MR^1. Similarly to **(iv)** in Theorem 5.1, **(v.1)** holds. Note that (x_M, y_M) is a jump point. Then by [18, Theorem 2.1, p.290], the locally invariant manifold M_ε, which is a stable manifold of the saddle (x_0^2, y_0^2), can extend to the boundary of the invariant region $\mathcal{A}$. Consequently, neither relaxation oscillations nor canard cycles with head appear. Hence, **(v.2)** holds. The statements **(v.3)** and **(v.4)** can be similarly proved by the method used in Theorem 5.3**(iii)**. Thus, **(v)** is proved.

To prove **(vi.1)**, by Theorem 5.1**(iv)**, near (x_i, y_i) Hopf bifurcations can take place by perturbing v, and the corresponding Hopf bifurcation curves $v_i^H(\cdot)$ are given by (5.12). Note that

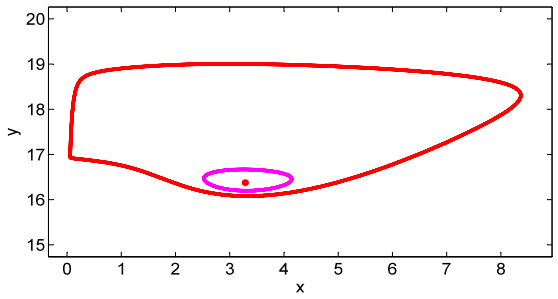

Fig. 8. A big limit cycle (the red cycle) encloses a small limit cycle (the mauve cycle). The red point indicates an equilibrium.

$D_{11}\psi_1(x_m, \lambda^0) < 0$, $D_{11}\psi_1(x_M, \lambda^0) > 0$, and $D_1\psi_2(x_i, \lambda^0, v^0) < 0$. Then $v_m^H(\varepsilon) > 0$ and $v_M^H(\varepsilon) < 0$ for sufficiently small ε, which implies that two Hopf bifurcations do not appear simultaneously. Thus, **(vi.1)** is proved. Similarly to **(v.3)** in this theorem, we can obtain **(vi.2)**. To prove **(vi.3)**, assume that $\mathcal{K}_m \neq \mathcal{K}_M$. Then by Lemma 5.2, two homoclinic orbits stated in **(vi.2)** cannot appear simultaneously. By (5.13) we obtain that canard cycles appear for the parameter v in the exponentially small interval of $v_i^c(\varepsilon)$. This together with $|v_m^c(\varepsilon) - v_M^c(\varepsilon)| = O(\varepsilon)$ yields that two canard cycles cannot appear simultaneously. The remaining statements can be proved by the similar way as the proof for **(v.4)**. Thus, **(vi)** is proved. Therefore, the proof is complete. □

5.3. Numerical examples

Now we give several concrete numerical examples to illustrate the obtained results as follows.

Example 5.1. Let the parameters a, b_1, b_2, c, ε and v satisfy $a = 0.01$, $b_1 = 20$, $b_2 = 0.1$, $c = 1$, $\varepsilon = 0.01$ and $v = 37.9$ in system (3.1). A numerical simulation shows that there exists a big limit cycle enclosing a small one. This indicates the coexistence of two limit cycles.

Example 5.2. Let the parameters a, b_1, b_2, c and ε be given by $a = 0.1$, $b_1 = 30$, $b_2 = 0.6$, $c = 1$ and $\varepsilon = 0.005$ in system (3.1). Then a canard explosion appears as the parameter v varies. See Figs. 9(a)–9(c).

6. Concluding remarks

We have studied the dynamics of the THTN model, which is a circadian oscillator model based on the dimerization and proteolysis of PER and TIM proteins in Drosophila. After giving a classification of all possible distributions of the equilibria, we obtain the existence of a bounded attractor in the first quadrant, the nonexistence of periodic solutions in the high degradation rate case, and the global dynamics in the low degradation rate case. These results are helpful for understanding the effects of the biophysical parameters on circadian oscillations in the THTN model.

More concretely, Theorem 4.1 shows that circadian oscillation disappears when the rate k_m of mRNA degradation is sufficiently high. As a result, the oscillatory behavior requires the rate k_m of mRNA degradation to be bounded. As stated in **(vi)** of Theorem 5.1, under some parameter conditions there exists the configuration of a big limit cycle enclosing a small one in the THTN model and a numerical example is presented in Fig. 8. This interesting phenomenon is called birhythmicity and suggests that depending on the different biological environments, the circadian oscillator exhibits different periodic behaviors. Theorems 5.1, 5.3 and 5.4 show that relaxation oscillations and canard cycles could also appear in the THTN model and Fig. 9 gives several concrete examples. For example, as shown in Fig. 9(c), when the concentration of mRNA is high, the total amount of PER protein increases to a high level in a short time. After that the concentration of mRNA decreases until it reaches a low level, and as a consequence the total amount of PER protein quickly decreases. Then the concentration of mRNA increases to a high level again. This process leads to the occurrence of a relaxation oscillation. Theorems 5.1, 5.3 and 5.4 also give the nonexistence of periodic solutions, and the existence of several complex oscillations including canard explosion and periodic solutions bifurcating from homoclinic orbits and heteroclinic orbits as the parameter v varies. These results suggest that the periods and the amplitudes of the circadian oscillations could be affected by the ratio of the rate of mRNA degradation to the rate of mRNA synthesis.

The results in the present paper could be also applicable to explain the numerical results in [8]. For example, assume that $v_m = 10k_m$ and take the values of other parameters as in [8, Table 1]. Then by [8, Figure 3B] and the formulas below (3.2), the THTN model with small k_m has exactly one equilibrium of type L^1 and no limit cycles when $K = 1$ (see **(i)** of Theorem 5.1). The equilibrium is of type M and one asymptotically stable relaxation oscillation arises when $K = 200$. This cycle is hyperbolic and not sensitive to the changes of parameters (see **(ii)** of Theorem 5.1). However, the equilibrium can be near the canard point when $K < 50$, and then canard explosion appears as the parameter K varies. So the limit cycle is sensitive to the changes of parameters (see **(iv)**, **(v)** and **(vi)** of Theorem 5.1). All of these results are consist with the numerical results in [8]. Consequently, our work is helpful to understand the effects of the biophysical parameters on oscillations in the THTN model.

It is also possible to understand the dynamics of the THTN model with the general rate k_m. By some changes, the THTN model can be transformed in a Liénard-like equation

$$\frac{dx}{dt} = y - \left((\varepsilon+1)(x^2+2x) + \frac{b_2x^2 + 2(b_1+b_2)x}{x^2+2x+a}\right),$$
$$\frac{dy}{dt} = 2\varepsilon(x+1)\left(\frac{v}{x^4+c} - \frac{b_2x^2 + 2(b_1+b_2)x}{x^2+2x+a} - x^2 - 2x\right),$$

where the parameters are defined as in system (3.1). Then the results on Liénard equations (see, for instance, [43,44]) can be applied to obtain the global dynamics of the THTN model in the general case. The Liénard-like structure for the THTN model could be helpful to investigate the effects of the model parameters on the periods of circadian oscillations.

CRediT authorship contribution statement

Shuang Chen: Conceptualization, Writing - original draft. **Jinqiao Duan:** Writing - review and editing, Supervision. **Ji Li:** Writing - review and editing.

Declaration of competing interest

The authors declare that they have no known competing financial interests or personal relationships that could have appeared to influence the work reported in this paper.

Acknowledgments

The authors would like to thank the editor and the anonymous referees for carefully reading the manuscript and providing valuable comments. The first author also thank Ke Shui from College of Life Science and Technology (HUST) for his valuable discussion. This work was partly supported by the NSFC, China grants 11531006, 11771449, 11771161, and the Science and Technology Project for Excellent Postdoctors of Hubei, China.

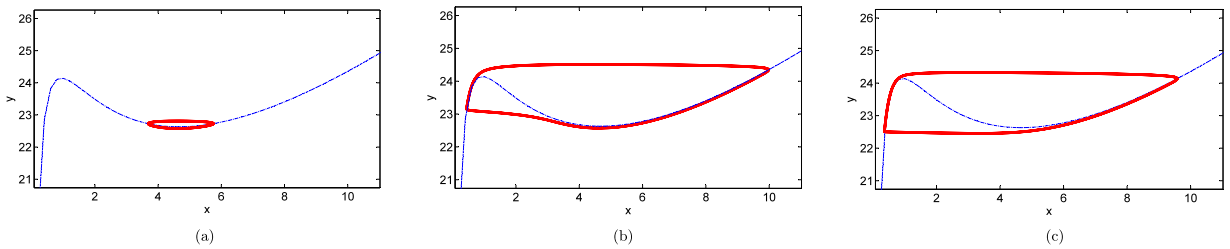

Fig. 9. Canard explosion in the slow–fast system (5.1). The dashed blue curves are the critical manifolds, the solid red cycles indicate periodic orbits. 9(a) Canard cycle without head arises when $v = 103$. 9(b) Canard cycle with head arises when $v = 98$. 9(c) Relaxation oscillation arises when $v = 53$.

Appendix A. Proof of Lemma 3.3

Before proving Lemma 3.3, we give the next auxiliary lemma.

Lemma A. *There exist positive parameters c and v such that the graph of ψ_2 passes a pair of points (ω_1, y_1) and (ω_2, y_2) with $\omega_1 < \omega_2$ in $\mathbb{R}^2_+$ if and only if the following properties hold:*

$$\frac{(\omega_1 - \phi(\omega_1))^2}{(\omega_2 - \phi(\omega_2))^2} < \frac{y_2}{y_1} < 1. \tag{A.1}$$

Proof. If the graph of ψ_2 passes points (ω_1, y_1) and (ω_2, y_2) with $\omega_1 < \omega_2$, then $0 < y_2 < y_1$ and

$$v = y_i(c + (\omega_i - \phi(\omega_i))^2), \quad i = 1, 2. \tag{A.2}$$

Clearly, the above equations have a unique solution (c, v) in the form

$$c = \frac{y_2(\omega_2 - \phi(\omega_2))^2 - y_1(\omega_1 - \phi(\omega_1))^2}{y_1 - y_2},$$
$$v = \frac{y_1 y_2((\omega_2 - \phi(\omega_2))^2 - (\omega_1 - \phi(\omega_1))^2)}{y_1 - y_2}.$$

By applying $c > 0$ and $v > 0$, we obtain (A.1). Thus, the sufficiency is proved.

If two points (ω_i, y_i) satisfy $\omega_1 < \omega_2$ and (A.1), then these equations in (A.2) have a unique solution (c, v) with $c > 0$ and $v > 0$. Thus, the necessity is proved. This finishes the proof. □

Now we prove Lemma 3.3 by the above lemma.

Proof of Lemma 3.3. By the monotonicity of the functions ψ_1 and ψ_2, we obtain that all possible combinations of intersection point sequences are as follows: *L*, *M*, *R*, *LM*, *MM*, *MR*, *LMM*, *LMR*, *MMM* and *MMR*. To complete the proof, it is only necessary to prove that all types shown in this lemma can be realized. Let the parameters $b_1 = b\widetilde{b}_1$ and $b_2 = b\widetilde{b}_2$, and the function φ be defined by $\varphi(x) = (\widetilde{b}_1\phi(x) + \widetilde{b}_2 x)/(a + x)$ for $x \geq 0$. Then $\psi_1(x) = b\varphi(x) + x$. By Lemma 3.1 there exist some a^*, b^* and $\widetilde{b}_i^*$ such that for some $x^* > 0$,

$$\frac{d\psi_1}{dx}(x^*) = b^*\frac{d\varphi}{dx}(x^*) + 1 = 0, \quad \frac{d^2\psi_1}{dx^2}(x^*) = b^*\frac{d^2\varphi}{dx^2}(x^*) = 0,$$
$$\frac{d^3\psi_1}{dx^3}(x^*) = b^*\frac{d^3\varphi}{dx^3}(x^*) > 0. \tag{A.3}$$

By the second equation, we observe that x^* is independent of b and only depends on the constants a and $\widetilde{b}_i$. Taking $c = c^* := (6u_*^5 + 5u_*^4)/(2u_* + 3)$, $u_* := \sqrt{1 + x^*} - 1$ and $v = v^* := (c^* + (x^* - \phi(x^*))^2)\psi_1(x^*)$, by Lemma 3.2 we have

$$\frac{d^2\psi_2}{dx^2}(x^*) = 0, \quad \psi_1(x^*) = \psi_2(x^*). \tag{A.4}$$

Let the parameters $a = a^*$, $\widetilde{b}_i = \widetilde{b}_i^*$ and $c = c^*$ be fixed. Consider the following equations

$$\frac{\partial\psi_1}{\partial x}(x, b, v) = 0, \quad \psi(x, b, v) = \psi_1(x, b, v) - \psi_2(x, b, v) = 0. \tag{A.5}$$

By (A.3) and (A.4) we have $(x, b, v) = (x^*, b^*, v^*)$ is a solution of (A.5). Since $b^* > 0$ and $\frac{\partial\psi_2}{\partial x}(x^*, b^*, v^*) < 0$, the matrix

$$\begin{pmatrix} \frac{\partial^2\psi_1}{\partial x^2} & \frac{\partial^2\psi_1}{\partial b\partial x} \\ \frac{\partial\psi}{\partial x} & \frac{\partial\psi}{\partial b} \end{pmatrix}_{(x^*, b^*, v^*)} = \begin{pmatrix} 0 & -\frac{1}{b^*} \\ \frac{\partial\psi_2}{\partial x}(x^*, b^*, v^*) & \varphi(x^*, b^*, v^*) \end{pmatrix}$$

is nonsingular. Thus by the Implicit Function Theorem, there exist two C^∞ functions

$$x(v) = x^* + \alpha_1(v - v^*) + O((v - v^*)^2),$$
$$b(v) = b^* + \alpha_2(v - v^*)^2 + O((v - v^*)^3),$$

such that $\frac{\partial\psi_1}{\partial x}(x(v), b(v), v) = 0$ and $\psi(x(v), b(v), v) = 0$ for small $|v - v^*|$, where the constants

$$\alpha_1 = -\frac{1}{\frac{\partial\psi_2(x^*, b^*, v^*)}{\partial x}(c^* + (x^* - \phi(x^*))^2)} > 0,$$
$$\alpha_2 = (\alpha_1 b^*)^2\frac{\partial^3\varphi(x^*, b^*, v^*)}{\partial x^3} > 0.$$

For sufficiently small $|v - v^*| > 0$ we have $b(v) > b^*$. By the first equation in (A.3) we obtain that $\frac{\partial\psi_1}{\partial x}(x^*, b^*, v^*) = -1/b^* < 0$, which implies that $\frac{\partial\psi_1}{\partial x}(x^*, b(v), v) = 1 - b(v)/b^* < 0$ for sufficiently small $|v - v^*| > 0$. From Lemma 3.1 it follows that the function $\frac{\partial\psi_1}{\partial x}(\cdot, b(v), v)$ has exactly two positive zeros $x_m(v)$ and $x_M(v)$ with $0 < x_m(v) < x^* < x_M(v)$. Note that the constant α_1 satisfies $\alpha_1 > 0$. Then $x(v)$ satisfies $x(v) = x_m(v)$ for $v < v^*$ and $x(v) = x_M(v)$ for $v > v^*$. By continuity we obtain that for sufficiently small $|v - v^*| > 0$, there is a constant $\varrho_2 > 0$ such that $x^* - \varrho_2 < x_m(v) < x^* < x_M(v) < x^* + \varrho_2$ and

$$\frac{\partial\psi_2}{\partial x}(x, b, v) \leq -2\varrho_2 < -\varrho_2 < \frac{\partial\psi_1}{\partial x}(x, b, v) \leq 0$$
$$\text{for} \quad x_m(v) \leq x \leq x_M(v).$$

Thus for small $v^* - v > 0$ (resp. $v - v^* > 0$), equation $\psi(x, b(v), v) = 0$ with respect to x has exactly one positive root $x = x_m(v)$ (resp. $x = x_M(v)$). Hence, the sequences L^0 and R^0 exist. Under the assumption that the sequence L^0 appears, let $(\omega_2, y_2) = (x_M, \psi_2(x_M))$ and $\omega_1 = x_m$ be fixed. By varying y_1, we obtain L^1 by decreasing y_1 slightly from $y_1 = \psi_1(x_m)$, and M by increasing y_1 slightly. Similarly, we can get the sequence R^1. Thus, the proof for **(i)** is obtained.

Take the parameters such that the intersection point sequence L^0 appears. Let two points (ω_1, y_1) and (ω_2, y_2) satisfy $(\omega_1, y_1) = (x_m, \psi_2(x_m))$ and $(\omega_2, y_2) = (x_M, \psi_2(x_M))$. Then by Lemma 3.3,

$$(x_m - \phi(x_m))^2/(x_M - \phi(x_M))^2 < \psi_2(x_M)/\psi_2(x_m) < 1,$$

which implies that for fixed $(\omega_1, y_1) = (x_m, \psi_2(x_m))$ and $\omega_2 = x_M$, the inequalities in (A.1) hold for each y_2 with $\psi_2(x_M) \leq y_2 < \psi_1(x_m) = \psi_2(x_m)$. In particular, set $y_2 = \psi_1(x_M)$. Then by Lemma 3.3 there exist some parameters c and v such that $\psi_1(x_m) = \psi_2(x_m)$ and $\psi_1(x_M) = \psi_2(x_M)$. Note that $\frac{d\psi_1}{dx}(x_i) = 0 > \frac{d\psi_2}{dx}(x_i)$, $i = m, M$, and ψ has at most three positive zeros. Then there exists exactly one point $x_3 \in (x_m, x_M)$ such that $\psi_1(x_3) = \psi_2(x_3)$. Thus the sequence L^0MR^0 appears and ψ_1 transversally intersects with ψ_2 at three different points. Varying y_2 slightly, we get the sequences L^0MM for $y_2 - \psi_1(x_M) < 0$ and L^0MR^1 for $y_2 - \psi_1(x_M) > 0$. By decreasing y_2 again, the sequence L^0M can be obtained. Hence, the sequences L^0M, L^0MM, L^0MR^0 and L^0MR^1 exist for suitable parameters. Similarly, we can obtain the sequences MR^0, MMR^0 and L^1MR^0 starting from R^0, the sequences L^1M, L^1MM and L^1MR^1 from L^1, the sequences MM, MMM and MMR^1 from M, and the sequence MR^1 from R^1. Thus, we give the proof for **(ii)** and **(iii)**. Therefore, the proof is now complete. □

Appendix B. Proof of (5.15)

We write system (5.14) as the form

$$\begin{aligned} \frac{dx}{dt} &= \bar{X}_2(x+y, v), \\ \frac{dy}{dt} &= \mu_1 y + \bar{Y}_2(x+y, v), \\ \frac{dv}{dt} &= 0, \end{aligned} \tag{B.1}$$

where $\bar{X}_2$ and $\bar{Y}_2$ denote X_2 and Y_2 with v^0 replaced by $v + v^0$, respectively. Note that system (B.1) has two zero eigenvalues and one nonzero eigenvalue μ_1 at the origin. Then by the center manifold theory [46, Section 1.3], system (B.1) has a C^3 center manifold $y = \tilde{y}(x, v)$ for sufficiently small $|x|$ and $|v|$. By a direct computation, the restriction of (B.1) to the center manifold has the expansion

$$\begin{aligned} \frac{dx}{dt} =& \frac{\varepsilon}{D_1\psi_1(x_0, \lambda^0) + \varepsilon} \times \left(\frac{1}{c^0 + (x_0 - \phi(x_0))^2} v \right. \\ &+ (D_{13}\psi_2(x_0, \lambda^0, v^0))(x + \tilde{y}(x, v))v \\ &+ \frac{1}{2}\left(D_{11}\psi_2(x_0, \lambda^0, v^0) - D_{11}\psi_1(x_0, \lambda^0)\right)(x + \tilde{y}(x, v))^2 \\ &\left. + \frac{1}{2}\left(D_{33}\psi_2(x_0, \lambda^0, v^0)\right)v^2 \right) + O(|(x, v)|^3), \\ \frac{dv}{dt} =& 0. \end{aligned} \tag{B.2}$$

Note that $D_{33}\psi_2(x_0, \lambda^0, v^0) = 0$ and $\tilde{y}(x, v) = O(|(x, v)|^2)$ for sufficiently small $|x|$ and $|v|$. Then we can write (B.2) as the form (5.15). This finishes the proof.

References

[1] J. Dunlap, Molecular bases for circadian clocks, Cell 96 (1999) 271–290.
[2] D. Forger, Biological Clocks, Rhythms, and Oscillations, MIT Press, Cambridge, MA, 2017.
[3] D. Gonze, Modeling circadian clocks: From equations to oscillations, Cent. Eur. J. Biol. 6 (2011) 699–711.
[4] J. Keener, J. Sneyd, Mathematical Physiology, in: Int. Appl. Math., vol. 8, Springer-Verlag, New York, 1998.
[5] J. Leloup, A. Goldbeter, A model for circadian rhythms in Drosophilia incorporating the formation of a complex between PER and TIM proteins, J. Biol. Rhythms 13 (1998) 70–87.
[6] B. Kloss, J.L. Price, L. Saez, J. Blau, A. Rothenfluh, C.S. Wesley, M.W. Young, The Drosophila clock gene double-time encodes a protein closely related to human casein kinase 1ε, Cell 94 (1998) 97–107.
[7] J.L. Price, J. Blau, A. Rothenfluh, M. Abodeely, B. Kloss, M.W. Young, Double-time is a novel Drosophila clock gene that regulates PERIOD protein accumulation, Cell 94 (1998) 83–95.
[8] J. Tyson, C. Hong, C. Thron, B. Novak, A simple model of circadian rhythms based on dimerization and proteolysis of PER and TIM, Biophys. J. 77 (1999) 2411–2417.
[9] S. Boie, V. Kirk, J. Sneyd, M. Wechselberger, Effects of quasi-steady-state reduction on biophysical models with oscillations, J. Theoret. Biol. 393 (2016) 16–31.
[10] A. Goeke, S. Walcher, E. Zerz, Determining "small parameters" for quasi-steady state, J. Differential Equations 259 (2015) 1149–1180.
[11] S. Chen, J. Duan, J. Li, Effective reduction of a three-dimensional circadian oscillator model, Discrete Contin. Dyn. Syst.-B, http://dx.doi.org/10.3934/dcdsb.2020349.
[12] P. Simon, A. Volford, Detailed study of limit cycles and global bifurcations in a circadian rhythm model, Internat. J. Bifur. Chaos 16 (2006) 349–367.
[13] D. Goussis, H. Najm, Model reduction and physical understanding of slowly oscillating processes: the circadian cycle, Multiscale Model. Simul. 5 (2006) 1297–1332.
[14] J. Jiang, Q. Liu, N. Lei, Theoretical investigation on models of circadian rhythms based on dimerization and proteolysis of PER and TIM, Math. Biosci. Eng. 14 (2017) 1247–1259.
[15] F. Dumortier, R. Roussarie, Canard Cycles and Center Manifolds, in: Mem. Amer. Math. Soc., vol. 577, Providence, 1996.
[16] G. Hek, Geometric singular perturbation theory in biological practice, J. Math. Biol. 60 (2010) 347–386.
[17] C.K.R.T. Jones, Geometric Singular Perturbation Theory, in: Dynamical Systems, Lecture Notes in Math., vol. 1609, Springer, Berlin, 1995, pp. 44–118.
[18] M. Krupa, P. Szmolyan, Extending geometric singular perturbation theory to nonhyperbolic points—fold and canard points in two dimensions, SIAM J. Math. Anal. 2 (2001) 286–314.
[19] M. Krupa, P. Szmolyan, Relaxation oscillation and canard explosion, J. Differential Equations 174 (2001) 312–368.
[20] C. Kuehn, Multiple Time Scale Dynamics, in: Appl. Math. Sci., vol. 191, Springer, Swizerland, 2015.
[21] S. Wiggins, Normally Hyperbolic Invariant Manifolds in Dynamical Systems, in: Appl. Math. Sci., vol. 105, Springer-Verlag, New York, 1994.
[22] N. Fenichel, Geometric singular perturbation theory for ordinary differential equations, J. Differential Equations 31 (1979) 53–98.
[23] B. Deng, G. Hines, Food chain chaos due to transcritical point, Chaos 13 (2003) 578–585.
[24] A. Ghazaryan, V. Manukian, S. Schecter, Travelling waves in the Holling-Tanner model with weak diffusion, Proc. A 471 (2015) 20150045, 16 pp.
[25] C. Li, H. Zhu, Canard cycles for predator–prey systems with Holling types of functional response, J. Differential Equations 254 (2013) 879–910.
[26] W. Liu, D. Xiao, Y. Yi, Relaxation oscillations in a class of predator–prey systems, J. Differential Equations 188 (2003) 306–331.
[27] C. Wang, X. Zhang, Canards, heteroclinic and homoclinic orbits for a slow-fast predator–prey model of generalized Holling type III, J. Differential Equations 267 (2019) 3397–3441.
[28] J. Albizuri, M. Desroches, M. Krupa, S. Rodrigues, Inflection, canards and folded singularities in excitable systems: Application to a 3D FitzHugh-Nagumo model, J. Nonlinear Sci. 30 (2020) 3265–3291.
[29] P. Carter, B. Sandstede, Fast pulses with oscillatory tails in the FitzHugh-Nagumo system, SIAM J. Math. Anal. 47 (2015) 3393–3441.
[30] B. de Rijk, A. Doelman, J. Rademacher, Spectra and stability of spatially periodic pulse patterns: Evans function factorization via Riccati transformation, SIAM J. Math. Anal. 48 (2016) 61–121.
[31] B. Eisenberg, W. Liu, Poisson-Nernst-Planck systems for ion channels with permanent charges, SIAM J. Math. Anal. 38 (2007) 1932–1966.
[32] J. Rubin, D. Terman, Geometric singular perturbation analysis of neuronal dynamics, in: Handbook of Dynamical Systems, Vol. 2, North-Holland, Amsterdam, 2002, pp. 93–146.
[33] E. Bossolini, M. Brøns, K.U. Kristiansen, A stiction oscillator with canards: on piecewise smooth nonuniqueness and its resolution by regularization using geometric singular perturbation theory, SIAM Rev. 62 (2020) 869–897.
[34] M. Desroches, J. Guckenheimer, B. Krauskopf, C. Kuehn, H. Osinga, M. Wechselberger, Mixed-mode oscillations with multiple time scales, SIAM Rev. 54 (2012) 211–288.
[35] Z. Du, J. Li, X. Li, The existence of solitary wave solutions of delayed Camassa–Holm equation via a geometric approach, J. Funct. Anal. 275 (2018) 988–1007.
[36] S. Jelbart, M. Wechselberger, Two-stroke relaxation oscillators, Nonlinearity 33 (2020) 2364–2408.
[37] N. Berglund, B. Gentz, Noise-Induced Phenomena in Slow-Fast Dynamical Systems: A Sample-Paths Approach, Springer-Verlag, London, 2006.

[38] G. Chen, J. Duan, J. Zhang, Slow foliation of a slow-fast stochastic evolutionary system, J. Funct. Anal. 267 (2014) 2663–2697.
[39] J. Ren, J. Duan, C.K.R.T. Jones, Approximation of random slow manifolds and settling of inertial particles under uncertainty, J. Dynam. Differential Equations 27 (2015) 961–979.
[40] W. Wang, A. Roberts, J. Duan, Large deviations and approximations for slow-fast stochastic reaction–diffusion equations, J. Differential Equations 253 (2012) 3501–3522.
[41] E. Benoit, J. Callot, F. Diener, M. Diener, Chasse au canards, Collect. Math. 31 (1981) 37–119.
[42] J. Grasman, Asymptotic Methods for Relaxation Oscillations and Applications, in: Appl. Math. Sci., vol. 63, Springer-Verlag, New York, 1987.
[43] F. Dumortier, J. Llibre, J. Artés, Qualitative Theory of Planar Differential Systems, Springer-Verlag, Berlin, 2006.
[44] Z. Zhang, T. Ding, W. Huang, Z. Dong, Qualitative Theory of Differential Equations, in: Transl. Math. Monographs, vol. 101, Amer. Math. Soc., Providence, 1992.
[45] J. Guckenheimer, P. Holmes, Nonlinear Oscillations, Dynamical Systems, and Bifurcations of Vector Fields, in: Appl. Math. Sci., vol. 42, Springer-Verlag, New York, 1983.
[46] J. Carr, Applications of Centre Manifold Theory, in: Appl. Math. Sci., vol. 35, Springer-Verlag, New York, 1981.
[47] S.N. Chow, J.K. Hale, Methods of Bifurcation Theory, Springer, New York, 1982.